Accepted Manuscript

Structure-activity relationships and mechanistic studies of novel mitochondria-targeted, leishmanicidal derivatives of the 4-aminostyrylquinoline scaffold

Matteo Staderini, Marta Piquero, María Ángeles Abengózar, Montserrat Nachér-Vázquez, Giulia Romanelli, Pilar López-Alvarado, Luis Rivas, Maria Laura Bolognesi, J. Carlos Menéndez

PII: S0223-5234(19)30218-1

DOI: https://doi.org/10.1016/j.ejmech.2019.03.007

Reference: EJMECH 11177

To appear in: *European Journal of Medicinal Chemistry*

Received Date: 28 December 2018

Revised Date: 8 February 2019

Accepted Date: 4 March 2019

Please cite this article as: M. Staderini, M. Piquero, Marí.Á. Abengózar, M. Nachér-Vázquez, G. Romanelli, P. López-Alvarado, L. Rivas, M.L. Bolognesi, J.C. Menéndez, Structure-activity relationships and mechanistic studies of novel mitochondria-targeted, leishmanicidal derivatives of the 4-aminostyrylquinoline scaffold, *European Journal of Medicinal Chemistry* (2019), doi: https://doi.org/10.1016/j.ejmech.2019.03.007.

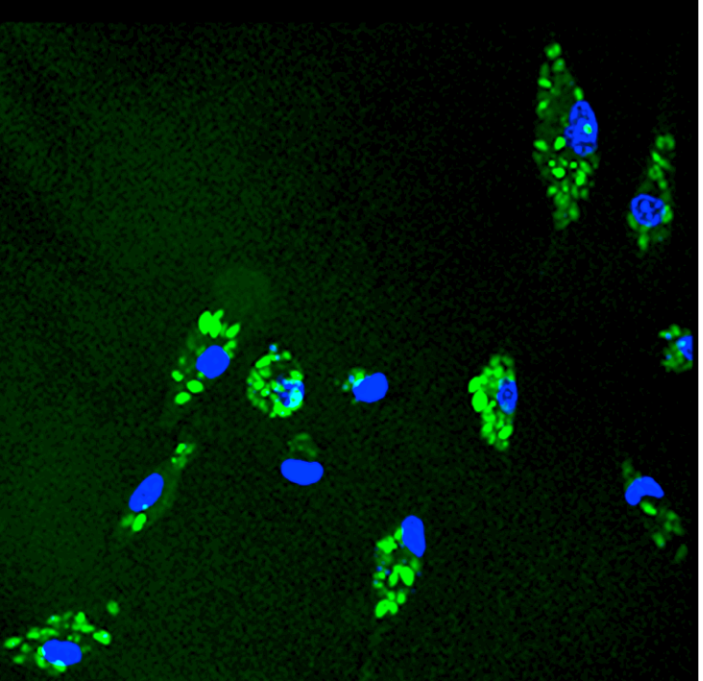

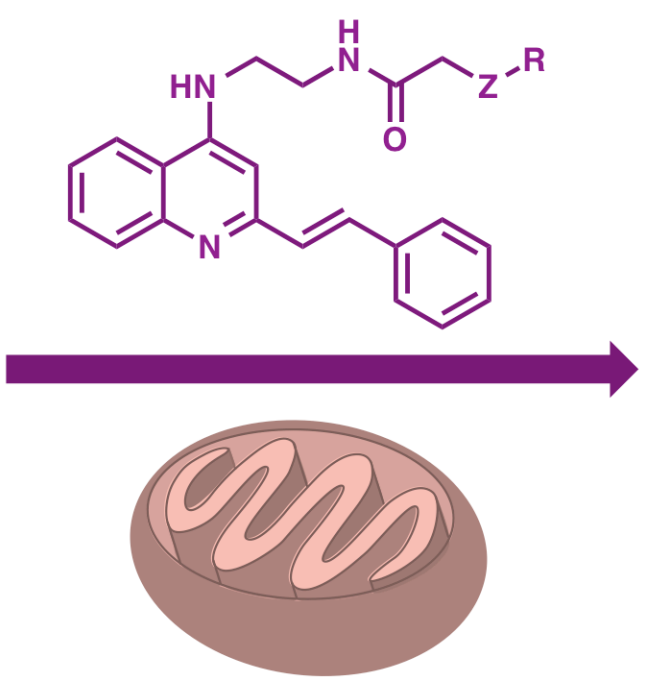
HN
H
N
Z
R
O
N

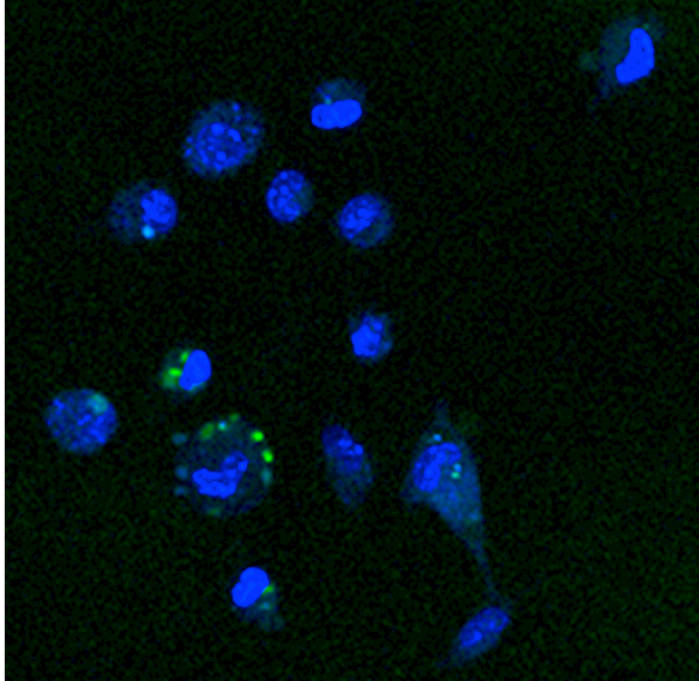

Structure-activity relationships and mechanistic studies of novel mitochondria-targeted, leishmanicidal derivatives of the 4-aminostyrylquinoline scaffold

Matteo Staderini,[1,‡] Marta Piquero,[1‡] María Ángeles Abengózar,[2,‡] Montserrat Nachér-Vázquez,[2] Giulia Romanelli,[1] Pilar López-Alvarado, [1] Luis Rivas,[2,*] Maria Laura Bolognesi,[3,*] J. Carlos Menéndez[1,*]

[1]Unidad de Química Orgánica y Farmacéutica, Departamento de Química en Ciencias Farmacéuticas, Facultad de Farmacia, Universidad Complutense, 28040 Madrid, Spain.

[2]Physico-Chemical Biology, Centro de Investigaciones Biológicas, CSIC, Ramiro de Maeztu 9, 28040 Madrid, Spain.

[3]Department of Pharmacy and Biotechnology, Alma Mater Studiorum – University of Bologna, Via Belmeloro 6, 40126 Bologna, Italy.

ABSTRACT

A new class of quinoline derivatives, bearing amino chains at C-4 and a styryl group at C-2, were tested on *Leishmania donovani* promastigotes and axenic and intracellular *Leishmania pifanoi* amastigotes. The introduction of the C-4 substituent improves the activity, which is due to interference with the mitochondrial activity of the parasite and its concomitant bioenergetic collapse by ATP exhaustion. Some compounds show a promising antileishmanial profile, with low micromolar or submicromolar activity on promastigote and amastigote forms and a good selectivity index.

KEY WORDS

Leishmanicidal compounds

4-Aminoquinolines

2-Styrylquinolines

Mitochondrial metabolism

INTRODUCTION

Among protozoal diseases, leishmaniasis is only superseded by malaria in terms of its impact on human health. Leishmaniasis, a neglected tropical disease, affects more than 2 million patients worldwide, most of them living in low-income countries in East Africa, India and South America.[1] Visceral leishmaniasis, caused by *Leishmania donovani*, *L. infantum* and *L. chagasi*, is fatal if untreated.[2,3]

No effective human leishmaniasis vaccine is available so far. Current pharmacological therapy is based on a few drugs, often with important side effects and/or high costs, the main ones being pentavalent antimonials (sodium stibogluconate, meglumine antimoniate), amphotericin B, particularly in a liposomal formulation, pentamidine, miltefosine and paromomycin (aminosidine). With the exception of oral miltefosine and topical paromomycin for the cutaneous ulcers, these drugs require parenteral administration with hospitalization of the patient. Furthermore, drug resistance threatens the effectiveness of chemotherapy.[4,5] Thus, there is an urgent need to discover new antileishmanial drugs.

In spite of the steady advances in the knowledge of *Leishmania* biology over the last two decades, their translation into the practical implementation of new drugs in the clinic has been poor.[6,7] This obeys to several reasons: (a) The return of investment in developing new leads from scratch for this disease is meager, as most of the patients live in poor-income areas. (b) Pharmacological treatment of leishmaniasis is intrinsically challenging, since an ideal therapy should provide a high effectiveness for all endemic regions, achieve cure in less than 10 days, be orally active, and cost less than $10 per course of treatment.[8]

Quinolines offer a high potential to develop effective and affordable oral treatments for leishmaniasis.[9] Among them, some 2-substituted derivatives have shown a high *in vitro* activity, low toxicity and a higher metabolic stability than their non-substituted counterparts.[10] The presence of a conjugated double bond on the side chain seems beneficial for activity, and in this context a class of styrylquinolines has shown activity at micromolar concentrations against *L. major* amastigotes infecting human monocyte-derived macrophages.[11-13] The quinoline derivative **1** (Figure 1), with an improved antileishmanial activity over the reference drug miltefosine and a good selectivity index (SI), entered the Drugs for Neglected Diseases initiative (DNDi) pipeline for *in vivo* evaluation.[14] Recently, the complex quinaldine derivative **2**, designed by pharmacophore-based virtual screening methods on the *Leishmania infantum* type 2 NADH dehydrogenase (NDH2), was experimentally confirmed to inhibit the enzyme and also to exhibit good activity against *L. infantum* axenic amastigotes and promastigotes.[15]

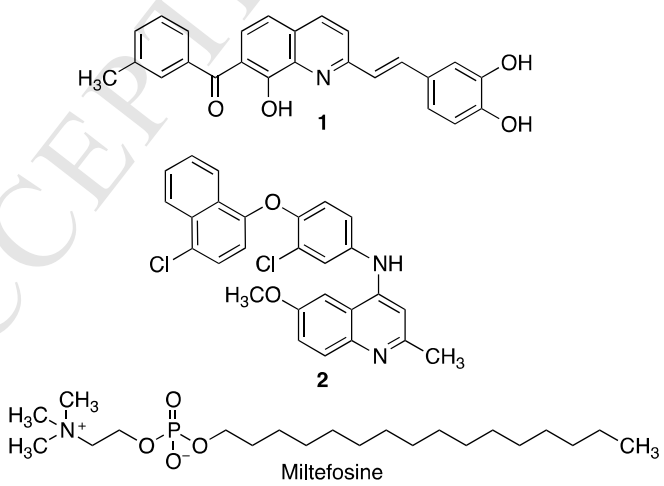

Figure 1. Structures of two leishmanicidal quinoline derivatives and the established anti-leishmanial drug miltefosine

RESULTS AND DISCUSSION

Compound design

There is much evidence showing that 8-aminoquinoline-based polyamines act on mitochondria. The most relevant example is sitamaquine (**3**), an orally active quinoline acting on the succinate dehydrogenase (complex II) at the *Leishmania* respiratory chain,[16,17] which has reached phase IIb clinical trials for the oral treatment of visceral leishmaniasis in India and Africa. Tafenoquine (**4**) is another quinoline bearing an 8-polyamino chain that targets the respiratory chain at the *Leishmania* mitochondrion, leading to an apoptosis-like death (Figure 2).[18] Other examples of antitrypanosomatid agents acting at mitochondria include naphthoquinone-cadaverine[19] and dibenzosuberyl–polyamine[20] hybrid compounds.

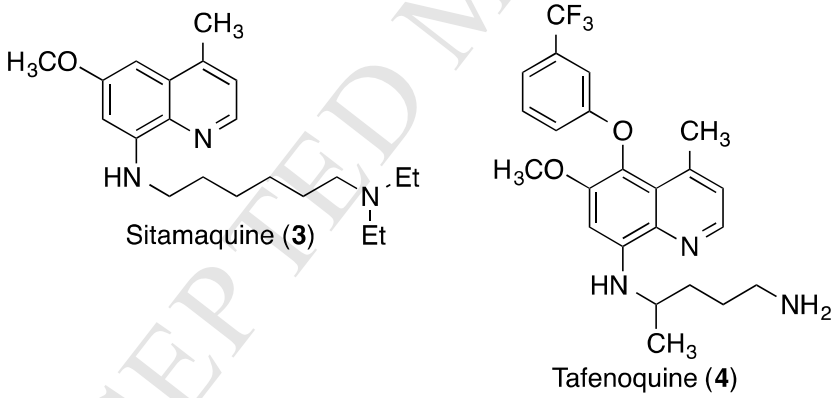

Figure 2. Structures of antileishmanial 8-aminoquinolines having mitochondrial targets.

Using the mitochondrial activity of 8-aminoquinoline-based polyamines as the starting point, we reasoned that an increase in the positive charge of the styrylquinoline nucleus would endow the resulting molecule with a more effective accumulation in the mitochondrion. This effect would be driven by the mitochondrial electrochemical potential ($\Delta\Psi_m$), which is the highest among

intracellular organelles. In *L. donovani* promastigotes $\Delta\Psi_m$ has a value of = -150 mV. Furthermore, mitochondrial dysfunction is particularly noxious for trypanosomatids such as *Leishmania*, which harbour a single mitochondrion, as their energy metabolism is based mostly on oxidative phosphorylation. Thus, glycolysis only accounts for 30% of ATP production in *L. donovani* promastigotes,[21] and a higher dependence of *L. mexicana* intracellular amastigotes on mitochondrial metabolism with respect to promastigotes has been reported.[22] Furthermore, glycolysis retooling to offset a dysfunctional mitochondrial function is quite limited, as demonstrated for tafenoquine-resistant *L. major* strains.[23] This is in contrast to higher eukaryotes, which may contain hundreds of mitochondria in a single cell.[24] Additionally, a drug targeting the mitochondrial synthesis of ATP ought to jeopardize the bioenergetic requirements of *Leishmania*, as 70% of them are fulfilled through oxidative phosphorylation. This is in line with a growing body of evidence that underscores the effectiveness of drugs acting on the *Leishmania* mitochondrion.[21]

To achieve our goal, we designed a new family of compounds obtained by introducing a polyamine chain at the C-4 position of the 2-styrylquinoline structure. The 4-aminoquinoline structural fragment would lead to an increased basicity at the heterocyclic nitrogen and, importantly, to a positive charge delocalized by resonance across the $N_1=C_2-C_3=C_4-NH_2$ fragment. This feature is expected to enhance the behavior of the molecule as a lipophilic cation, key for its potential-driven transport across the inner mitochondrial membrane and accumulation into the mitochondrial matrix.[25] Surprisingly, 4-aminoquinolines, a mainstay in other fields of antiprotozoal therapy (*e.g.* in the case of malaria), have received scant attention in leishmaniasis.[15,26] On the other hand, the presence of

two amino groups in the polyamine chain could lead to an increased compound retention by the acidic environment of the phagolysosomes, where the amastigote forms multiply.[27] The design of our compounds sought to find out which of these two effects takes precedence. Thus, the choice of substituents at the end of the polyamine chain (represented by Z) aimed to modulate the basicity of the nitrogen atoms at C-4, and it was also guided by their presence in previously reported antileishmanial compounds, as in the case of the amodiaquine analogue **21**.[28,29] and indolylquinoline **22**.[30] A number of compounds representing structural fragments of our proposed structures, namely **17-20** and 2-styrylquinoline **23**, devoid of the C-4 substituent, served as a controls.

The main features of the criteria used for the design of our compounds are summarized in Figure 3, and the structures of the styrylquinoline derivatives studied (compounds **11a-15b**) are shown in Figure 4.

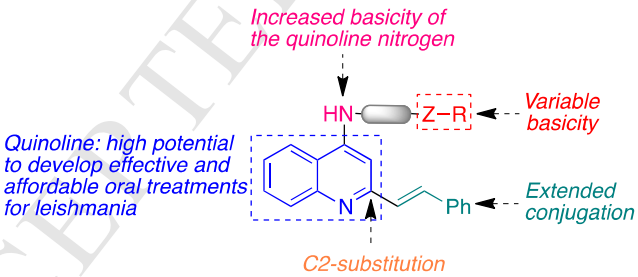

Figure 3. A summary of our criteria for compound design

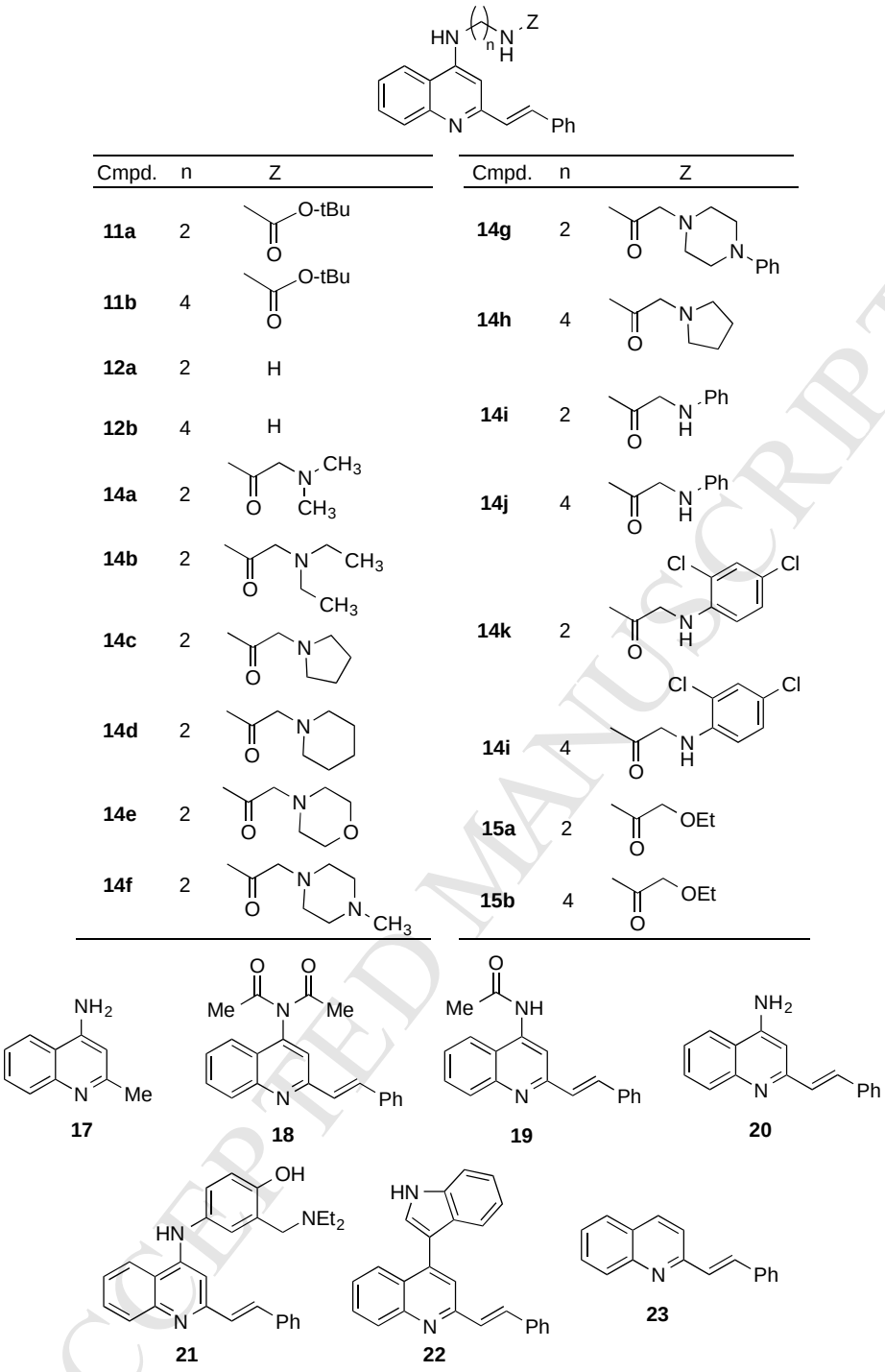

Figure 4. Structures of the compounds studied in this work.

Preliminary ADME-tox computational studies of the designed compounds were carried out using SwissADME.[31] For all our compounds, a high gastrointestinal absorption was predicted, which is an important factor for oral bioavailability. Moreover, only compounds **14** and **22** were found to violate Lipinski's rule of five,

and only compound **21** showed a PAINS alert. See the full details of this study in Table S2.

Synthesis

Our synthetic strategy involved the initial generation of a functionalized styrylquinoline core, followed by its decoration with the selected basic chains at C-4. We started with the preparation of the known 4-chloro-2-styrylquinoline **6** by two alternative methods, which differ from the previous one found in the literature[32] and are summarized in Scheme 1. For route A, the commercially available 4-chloroquinaldine **5** was submitted to a microwave-promoted aldol condensation with benzaldehyde in the presence of zinc chloride. Alternatively (route B), a similar aldol condensation of the known 2-methylquinolin-4(1*H*)-one, this time in the presence of acetic anhydride, afforded compound **8**, which was treated with $POCl_3$ to furnish **6**.

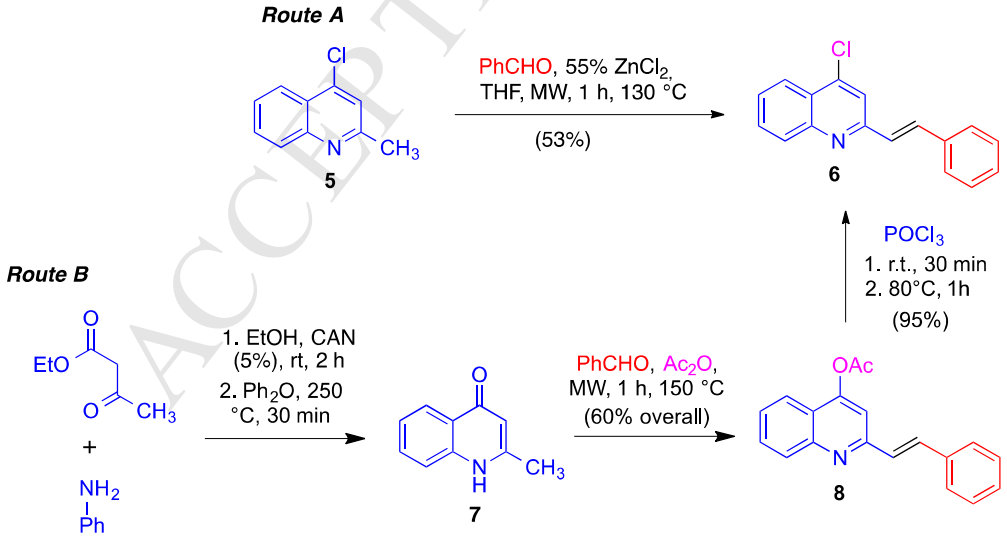

Scheme 1. Synthesis of the starting material, compound **6**

After preparation of the suitable monoprotected polyamine chains (**10a** and **10b**), compound **6** was treated with an excess of these compounds in the presence of phenol to promote a nucleophilic aromatic substitution that yielded compounds **11a** and **11b**. These intermediates were deprotected using a solution of trifluoroacetic acid in methanol, giving **12a** and **12b**. Compound **12a** was also obtained by treating **6** with a large excess of ethylenediamine under focused microwave irradiation, conditions that were designed to avoid a competing double substitution. In the case of compound **12b**, this procedure was not feasible due to the impossibility of evaporating the diamine in excess. Compounds **12a** and **12b** were then transformed into the corresponding halides **13** by treatment with bromoacetyl bromide at -5 °C. In the final step, the reaction of **13** with a variety of amines under microwave irradiation in the presence of Cs_2CO_3 yielded the target compounds **14 a**-**h**. Similarly, the treatment of **13** with ethanol under the same reaction conditions gave compounds **15 a-b** (Scheme 2).

This method failed for the preparation of the aniline derivatives **14i-l**, owing to the low nucleophilicity of aromatic amines. In search for an alternative procedure, we prepared *N*-arylglycine derivatives, having the desired aryl substitution patterns (compounds **16a-b**), by reacting the suitable anilines with ethyl bromoacetate in the presence of sodium hydride, followed by ester saponification. Compounds **16a-b** were then coupled to the previously mentioned primary amines **12a-b** using EDC/HOAt as activating agents (Scheme 3).

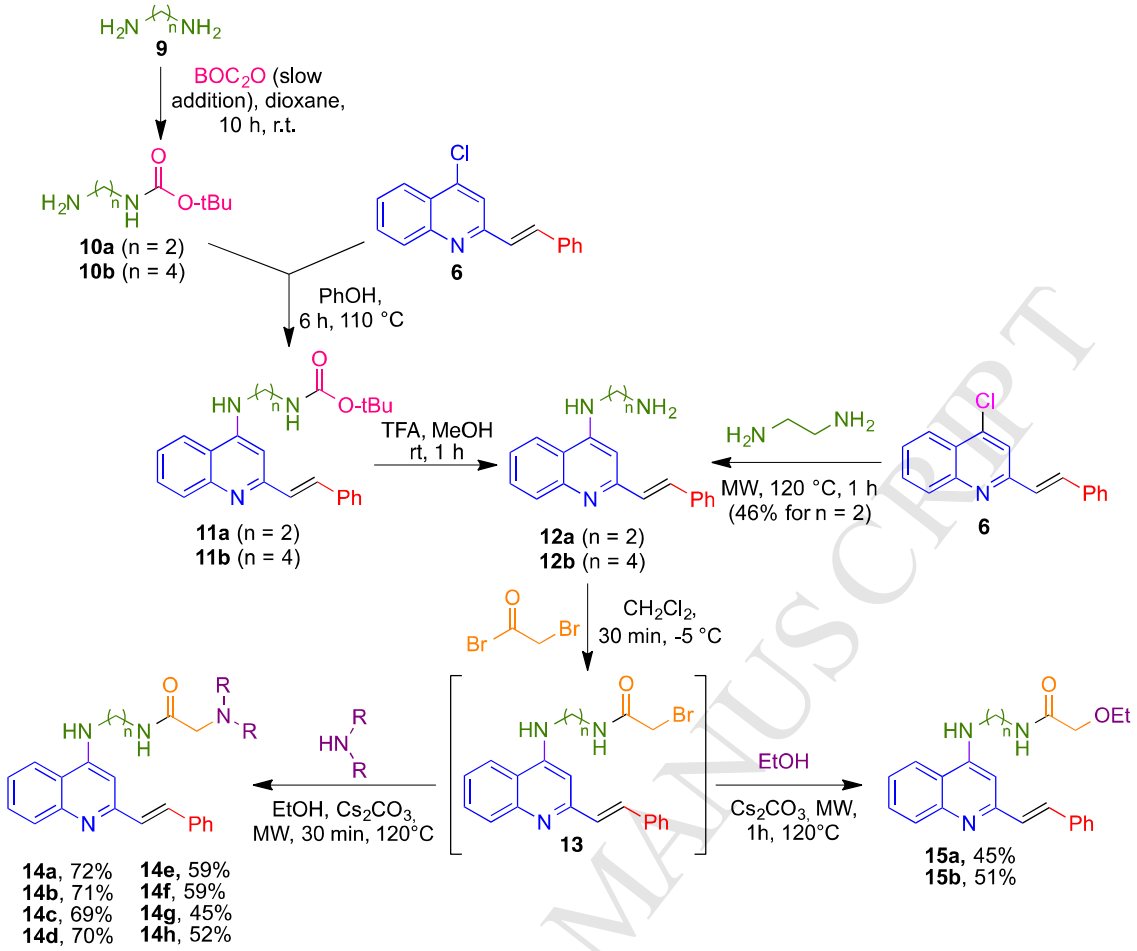

Scheme 2. Synthetic route for the preparation of compounds **14a-h** and **15a-b**

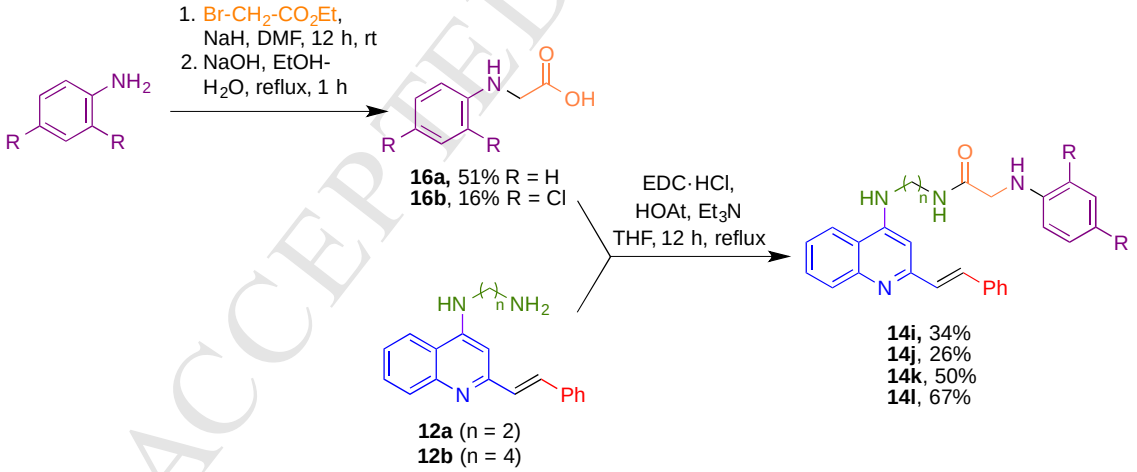

Scheme 3. Synthetic route for the preparation of compounds **14i-l**.

In order to evaluate the influence of the polyaminoalkyl chain, the reference compound **20** was designed. For its preparation, the commercially available 4-amino-2-methylquinoline **17** was condensed with benzaldehyde in the presence of

zinc chloride and acetic anhydride, giving a mixture of compounds **18** and **19**, at different levels of *N*-acetylation. Although both compounds were purified for their biological evaluation, for the preparation of the target compound **20,** the mixture was submitted to amide hydrolysis using KOH dissolved in methanol-water under microwave irradiation (Scheme 4).

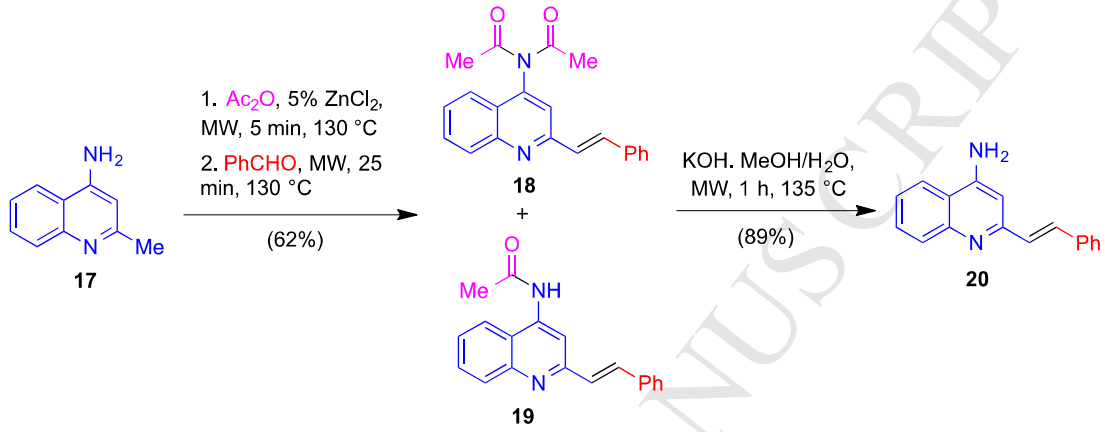

Scheme 4. Synthetic route for the preparation of compound **20**.

The amodiaquine analogue **21** and the 4-(3-indolyl) derivative **22** were prepared using our reported conditions for C-N and C-C bond formation at the quinoline C-4 position, that involve the use of $InCl_3$ as a Lewis acid catalyst, under focused microwave irradiation.[33] By applying this method, treatment of 4-chlorostyrylquinoline **6** with 4-amino-2-(diethylaminomethyl)phenol or indole afforded compounds **21** and **22** in 54% and 58% yield, respectively (Scheme 5). Finally, the reference non-substituted 2-styrylquinoline **23** was synthesized following a known method based on the use of a type II vinylogous Povarov reaction.[34]

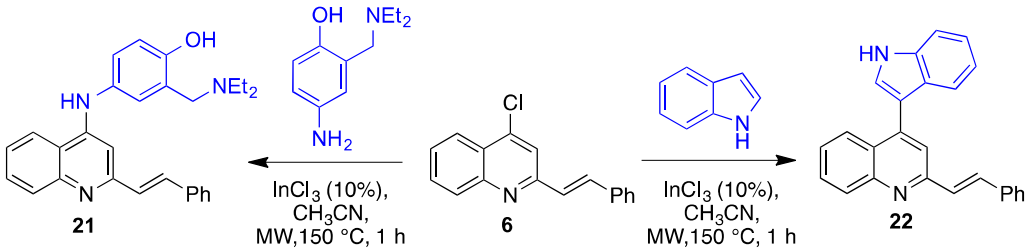

Scheme 5. Synthetic route for the preparation of compounds **21** and **22**

Antileishmanial activity studies

In order to test the mitochondrial tropism of our compounds, we decided to use *Leishmania* promastigotes as a model system. At this stage of the parasite life cycle, mitochondrial synthesis accounts for nearly 70% of the total production of ATP,[21,24,35] and therefore the study of promastigote forms facilitates the identification of drugs affecting mitochondrial ATP production. Thus, the activity of compounds **11**-**23** was evaluated against *Leishmania donovani* promastigotes (strain MHOM/SD/00/1S-2D) in a phenotypic screening. All compounds, except the control **23**, inhibited the proliferation of this parasite form, showing IC_{50} values in the 0.2 – 35.1 μM range (Table 1). Notably, most of our compounds were more potent than **2**, a marketed antileishmanial drug.[36] The low activity (IC_{50} > 50 μM) of 2-styrylquinoline **23**, devoid of the amino tail at its C-4 position, showed that the latter structural fragment is critical for activity, and the comparison of compounds **18** and **19** with **20** confirmed the starting hypothesis that the basicity of the quinoline core is critical for activity. Moreover, the lower activity of compound **17** compared to **20** proved the importance of the styryl fragment. This was further underscored by comparison of compound **12a** with a related quinoline derivative lacking the styryl substituent, namely 7-chloro-4-(2-aminoethylamino)quinoline, which showed no activity against *L. amazonensis* and *L. brasilensis* promastigotes.[37]

Motivated by these promising results, we studied the activity of our compounds against *Leishmania pifanoi* axenic amastigotes (strain MHOM-ET-67/L82), with the results summarized in Table 1. The choice of this model was driven by the extensive documentation for this axenic line and its similarity with those amastigotes obtained from lesions.[38] A good inhibition of amastigote proliferation was found for most compounds and some of them, namely **14b** and **14c**, showed submicromolar IC_{50} values, being only slightly less potent than our miltefosine standard. It is worth noting that the amastigote stages had similar or even higher sensitivity towards our styrylquinolines in comparison with promastigotes. This is a relevant finding, as there are remarkable differences between these two forms with respect to biochemical and mitochondrial bioenergetics, and many anti-leishmanial compounds active on promastigotes fail to inhibit amastigotes.[39] The mammalian cell toxicity of compounds **11-23** was then assessed on macrophages, the host cell for *Leishmania*, using the tumoral murine macrophage cell line J774, a model extensively used to test drug activity on intracellular amastigotes while avoiding the activation of the macrophages by phorbol esters required for the differentiation of promonocytic and monocytic cell lines.[40] The IC_{50} values thus obtained were used to calculate a selectivity index (SI). As shown in Table 1, many of our compounds showed some macrophage toxicities at leishmanicidal concentrations, and had selectivity indexes below 10. However, **14a**, **14c**, **14k** and **15a**, displaying potent antileishmanial activities, showed respectable SI values, allowing to regard them as relatively selective, nontoxic chemotypes. It is interesting to note that, in those cases allowing comparison (**14c** *vs.* **14h**, **14i** *vs.* **14j**, **14k** *vs.* **14l**, **15a** *vs.* **15b**), the two-carbon spacer chain led to better results than the four-carbon spacer. While several compounds had good activity against

amastigotes, **14k** had the best overall profile, with micromolar activity against amastigotes and a SI above 41.6. The fact that this is the compound with the least basic side chain, but carrying the 4-amino substituent, suggests that protonation of the quinoline moiety is important for activity and has implications for the design of future antileishmanial quinoline derivatives.

Table 1. Leishmanicidal activities, cytotoxicities and selectivity indexes of compounds **11-23** and miltefosine (2)[a]

Cmpd.	*L. donovani* promastigotes, IC_{50} (μM)	*L. pifanoi* amastigotes, IC_{50} (μM)	J774, IC_{50} (μM)	SI[b]
11a	0.45 ±0. 32	4.3 ± 1.2	6.6 ± 1.8	4.7
11b	0.56 ±0.12	4.9 ±0.8	3.7 ± 0.5	0.8
12a	2.4 ±0.3	>50	4.6 ± 0.2	<0.1
12b	0.44 ± 0.1	> 25	6.6 ± 0.6	<0.3
14a	1.6 ± 0.0	1.1 ± 0.1	15.0 ±2.7	13.6
14b	1.6 ± 0.0	0.9 ± 0.1	0.7 ± 0.1	0.8
14c	2.1 ± 0.2	0.9 ± 0.1	12.5 ±3.5	13.9
14d	2.1± 0.2	1.2 ± 0.1	4.7 ± 1.0	3.4
14e	1.3 ± 0.1	> 25	> 50	2.0
14f	3.5 ± 0.3	3.5 ± 0.3	34 ± 1.2	9.7
14g	2.1 ± 0.1	1.5 ± 0.2	4.5 ± 0.2	3.0
14h	0.2 ± 0.0	5.3 ± 0.8	7.1 ±1.0	1.4
14i	3.3 ± 0.8	4.3 ± 2.4	7.8 ± 1.2	1.8
14j	1.6 ±0.4	6.9 ± 1.5	3.3 ± 0.8	0.48
14k	8.4 ± 2.4	1.2 ± 0.8	>50	> 41.6
14l	2.1 ± 0.2	12.3 ± 3.2	7.3 ± 1.2	0.6
15a	3.4 ± 0.2	1.6 ± 0.4	22.2 ± 4.6	13.8
15b	1.06 ± 0.11	4.5 ± 1.2	7.2 ± 0.9	1.6
17	10.9 ± 2.2	> 50	> 50	-
18	35.1 ± 4.6	13.4 ±3.8	>25	>1.86
19	ND.	9.5 ±2.2	>25	>2.6
20	0.5 ±0.1	8.9 ±2.0	4.4 ± 0.2	0.5

21	9.6 ± 0.4	9.0 ± 0.6	37 ± 2.2	4.1
22	1.5 ± 0.6	1.0 ± 0.5	4.1 ±1.0	4.1
23	>50	> 50	> 50	ND
2	4.4 ± 0.7	6.2 ± 1.6	> 50	> 8.1

[a] All results are representative of two experiments performed independently. [b] SI = IC_{50}(J774)/IC_{50} (*L. pifanoi* amastigotes).

We next planned to investigate the leishmanicidal activity of one selected compound against macrophage cells infected with *L. pifanoi* amastigotes. Several of our compounds (**14a**-**d**, **14g**, **14k**, **15a**, **22**) had shown similar inhibitory activities against amastigote forms in the low micromolar level and were therefore considered suitable for these studies. Among them, we chose **15a**, due to its better synthetic accessibility. Murine peritoneal macrophages are terminally differentiated non-transformed cells, and were used instead of J774 in order to avoid replication of the host cells, as well as additional toxicity due to the tumoral character of the J774 line. Parasites were fluorescently labelled with carboxyfluorescein succinimidyl ester (CFSE) prior to the infection to facilitate their fluorescent visualization inside the macrophages. The infection index (number of parasites/macrophage) decreased from 5.3 ± 2.5 in untreated macrophages to 1.6 ± 0.8 after incubation with **15a** at 10 μM concentration. A visual assessment of this activity is shown in Figure 4.

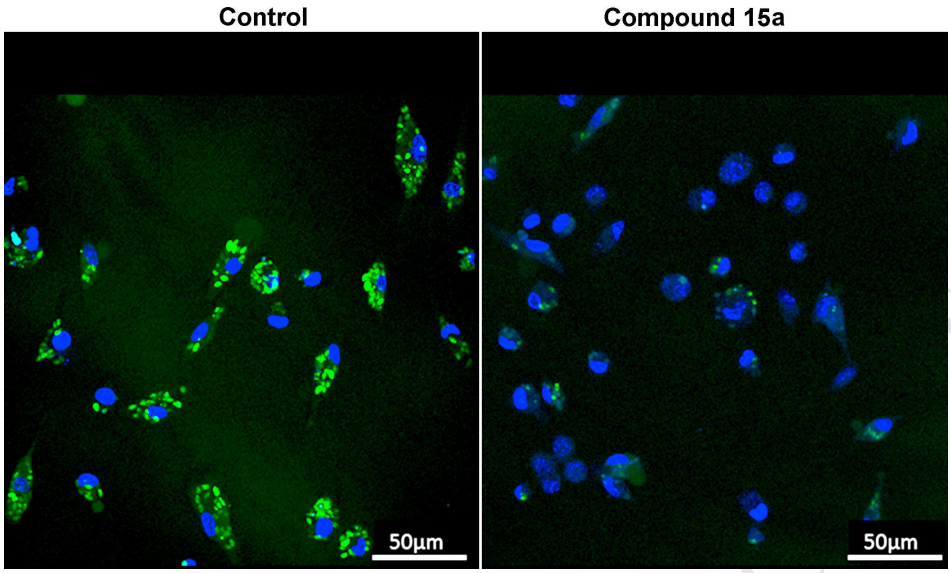

Figure 4. Leishmanicidal activity of **15a** on murine peritoneal macrophages infected with *L. pifanoi* amastigotes. Infected macrophages were treated with **15a** (10 µM) for 12 h. Infection was observed under a confocal microscope. Amastigotes were prelabelled intracellularly with CFSE (λ_{exc} = 488 nm/ λ_{em} = 520 nm, green fluorescence). Intracellular nucleic acids were stained with DAPI (λ_{exc} = 350 nm/ λ_{em} = 460 nm, blue fluorescence).

Mechanistic studies

The proposed mitochondrial involvement in the leishmanicidal mechanism of our compounds was corroborated by two complementary approaches. First, as the mitochondrion is the main contributor to ATP synthesis in *Leishmania*, the variation in the levels of intracellular ATP with our compounds was monitored using *L. donovani* promastigotes from the 3-Luc strain.[41] These parasites express a cytoplasmic form of firefly luciferase that is episomally encoded. The free cytoplasmic ATP was the limiting substrate for *in vivo* luminescence, as luciferin supply was in excess, administered as the caged membrane-permeable substrate DMNPE-luciferin. This strategy has been previously employed to characterize the involvement of mitochondrion in leishmanicidal mechanisms.[19,42] At 50 µM concentration, all studied compounds caused a decrease in luminescence to a variable extent (Table S1). The dependence of this effect with concentration is

represented in Figure S1 for the case of **15a**, which showed a threshold of 3.12 μM. The inhibition endpoint was reached in less than 5 min after compound addition. Inhibition of luciferase *in vitro* at the highest concentration (50 μM) was lower than 2% in every case (data not shown). This dramatic drop in ATP levels can be feasibly due either to permeabilization of the cell membrane or to mitochondrial dysfunction. To check the first mechanism, we studied whether a selection of our compounds were able to induce plasma membrane permeabilization. To this end, the entry of the vital dye SYTOX Green, included in the incubation medium, was monitored after addition of the styrylquinoline by examining the increase in its fluorescence due to its binding to intracellular nucleic acids. Fully permeabilized cells were obtained by addition of 0.1% Triton X-100. None of the compounds was found to alter the plasma membrane permeability (Figure S2).

Once plasma membrane permeabilization was discarded, loss of mitochondrial functionality was addressed. Variations in the mitochondrial electrochemical potential ($\Delta\Psi_m$), essential to drive ATP synthesis, were monitored after addition of selected compounds. The accumulation of rhodamine 123, driven by $\Delta\Psi_m$, was tested by flow cytometry (Figure S3). Compounds **14d**, **14h**, and **15a** showed the highest inhibition and were selected for a concentration dependency study. At 25 μM, these styrylquinolines markedly decreased rhodamine 123 levels, matching the decrease induced by 20 mM KCN, a control for full mitochondrial depolarization. The combined results show that exposure to our compounds induces mitochondrial dysfunction.

To further corroborate our initial hypothesis, the mitochondrial localization of compound **15a** inside *Leishmania* was assessed on axenic amastigotes by confocal microscopy. At 20 μM, the accumulation of **15a** appeared as a punctuated

fluorescence pattern (Figure 5, panel A). Fluorescence was considerably inhibited upon addition of 1 mM KCN, a concentration able to fully depolarize mitochondrion while preserving parasite viability,[43] underscoring the role of $\Delta\Psi_m$ in the intracellular compound accumulation. In a double-labeling experiment, **15a** was incubated together with the fluorescent mitochondrial probe MitoTracker Red (MTR). A high degree of overlapping for both probes was observed (Figure 5, panel B).

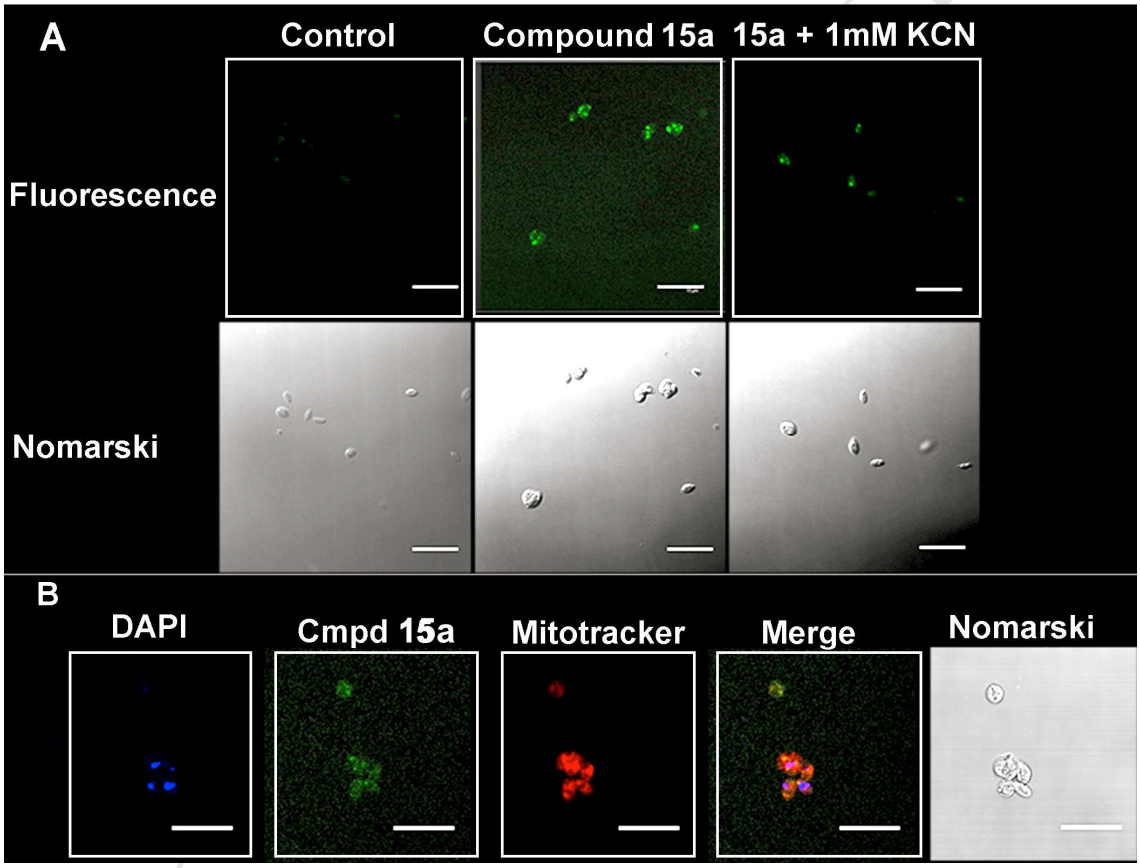

Figure 5. Confocal microscopy of *L. pifanoi* axenic amastigotes incubated with compound **15a**. A: Uptake and intracellular distribution of **15a** in *L. pifanoi* amastigotes. Parasites were incubated with **15a** at 20 µM for 1 h and observed by confocal microscopy. Amastigotes with a depolarized mitochondrion were obtained by incubation with 1 mM KCN 15 min prior to addition of **15a**. B: Co-localization of **15a** with MTR. Amastigotes were successively labeled with 0.05 µM MTR, 20 µM **15a**, and 5 µg/ml DAPI. Fluorescence settings: λ_{exc} = 488 nm/λ_{em} = 520 nm for **15a**; λ_{exc} = 350 nm/ λ_{em} = 460 nm for DAPI; and λ_{exc} = 570 nm/ λ_{em} = 590 nm for MTR. Fluorescence overlapping for **15a** and MTR was expressed as Pearson coefficient (r); r = 0.53 ± 0.03. Magnification bar = 15 µm.

As the *Leishmania* mitochondrion is involved in programmed cell death,[44] cells at the late stages of apoptosis, characterized by a fragmented chromatin, can be identified by a lower degree of staining with propidium iodide (subG1 population). As shown in Figure S4, the subG1 population for *L. donovani* promastigotes incubated with **15a** (4.3%) was similar to untreated parasites (4.6%), whereas upon treatment with **2**, an inducer of apoptosis–like process in *Leishmania*, it reached 22.5%.[45] The concentration of **15a** in this experiment (20 μM) exceeded that required for a full elimination of the promastigotes. Therefore, compound **15a** is not an apoptosis inducer.

The morphological damage inflicted by **15a** on *L. donovani* promastigotes was assessed by transmission electron microscopy (Figure 6). Parasites treated with **15a** showed a swollen mitochondrion and strong vacuolization of the cytoplasm, together with the appearance of distended acidocalcisomes, identified by the presence of electron-dense material, mostly Zn^{2+} and Fe^{2} in these organelles. Acidocalcisomes, in fact, work as an acidic storage for divalent (Ca^{2+}) and heavy metal (Zn^{2+} and Fe^{2+}) cations, due to their high polyphosphate content.[46] In view of this result, the role of acidocalcisomes as a feasible target of **15a** was further investigated, by using acridine orange (AO) dye as an acidocalcisome pH indicator.[47] Not unexpectedly, the intraorganellar acidic pH was quenched by **15a**, but not by the less basic (and less active) **23**, according to the quantitative differences in fluorescence of AO inside the parasites (Figure S5, panel A) and visualization by confocal microscopy (Figure S5, panel B). Nevertheless, the importance of acidocalcisomes in terms of the leishmanicidal mechanism of **15a** is questionable, for two reasons. First, the polyphosphate content was not reduced after treatment with **15a** (5 μM), as evaluated by DAPI fluorescence. Second,

acidocalcisomes were discarded as a target for tafenoquine (**4**), even though it caused a more severe dysfunction than **15a**, including a decrease in polyphosphate content, because parasites deficient in acidocalcisome biogenesis were equally susceptible to **4**.[48]

These studies notwithstanding, additional targets for styrylquinolines cannot be ruled out, as frequently found for other antileishmanial drugs, such as miltefosine[49,50] or paromomycin.[51,52] Even for drugs with traditionally well-established lethal mechanisms, additional effects are often uncovered, mostly through analysis of drug-resistant strains. A case in point is amphotericin B; its lethal mechanism is mostly based on the plasma membrane permeabilization of the parasite by formation of an aqueous pore. Nevertheless, subtle additional effects contributing to its lethal action have been recently described, including triggering of signal transduction pathways and induction of oxidative stress, not only for pathogens, but also for their host cells.[53]

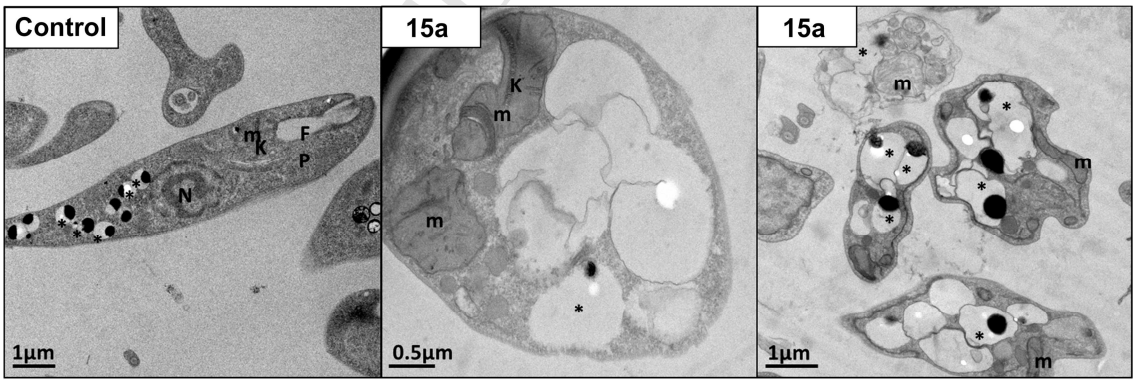

Figure 6. Transmission electron microscopy of *L. donovani* promastigotes treated with **15a** (5 μM). Legend: (K) kinetoplast, (M) mitochondrion, (N) nucleus, (FP) flagellar pocket, (*) acidocalcisome.

CONCLUSIONS

Our results confirm the mitochondrial druggability by aminoquinolines, adding the 4-amino-2-styrylquinoline family to the previously known 8-aminoquinolines, that also kill *Leishmania* by inhibition of mitochondrial functionality.[17,18] Some of our compounds, especially **14a**, **14c**, **14k** and **15a**, exhibit a promising antileishmanial profile, with a similar activity against promastigote and amastigote forms to the drug miltefosine, used as a reference, and a good selectivity index.

EXPERIMENTAL SECTION

Chemistry

General experimental information

All reagents (Aldrich, Fischer, Alpha Aesar, SDS) and solvents (Scharlau, Fischer, SDS) were of commercial quality and were used as received. Reactions under microwave irradiation were carried out in a CEM Discover SP microwave reactor. Reactions were monitored by thin layer chromatography on aluminium plates coated with silica gel and fluorescent indicator (Macherey-Nagel Xtra SIL G/UV254). Separations by flash chromatography were performed on silica gel (Scharlau 40–60 μm, 230–400 mesh ASTM) or neutral alumina (Merck S22). Melting points were determined using a Stuart Scientific apparatus, SMP3 Model, and are uncorrected. Infrared spectra were recorded with an Agilent Cary630 FTIR spectrophotometer with a diamond accessory for solid and liquid samples. NMR spectroscopic data were recorded using a Bruker Avance 250 spectrometer operating at 250 MHz for ^{1}H NMR and 63 MHz for ^{13}C NMR maintained by the NMR facility of Universidad Complutense (CAI de Resonancia Magnética Nuclear);

chemical shifts are given in ppm and coupling constants in Hertz. High-resolution mass spectra (HRMS) were recorded on a mass spectrometer fitted with an electrospray detector (ESI) by the mass spectral facility of Universidad Complutense (CAI de Espectrometría de Masas) and elemental analyses were determined by the microanalysis facility of Universidad Complutense (CAI de Microanálisis Elemental), using a Leco 932 combustion microanalyzer. The synthesis of compounds **6** and **10** is described in the Supporting Information.

General procedure for the synthesis of protected polyamino styrylquinolines (11)

(E)-4-Chloro-2-styrylquinoline **6** (1 eq), the corresponding monoprotected diamine **10** (1.5 eq) and phenol (6 eq) were placed in a round bottom flask and stirred at 110 °C for 6 h. The reaction mixture was basified with an aqueous solution of NaOH (5M) and extracted with ethyl acetate (3 × 10 ml). The combined organic phases were dried with anhydrous Na_2SO_4 and evaporated. The resulting crude was purified by flash chromatography through a silica gel column eluting with hexane: ethyl acetate (2:1, v/v) as the mobile phase to give the desired products.

***tert*-Butyl (*E*)-(2-((2-styrylquinolin-4-yl)amino)ethyl) carbamate (11a).** Prepared from *(E)*-4-chloro-2-styrylquinoline **6** (0.654 g, 2.46 mmol), *tert*-butyl (2-aminoethyl) carbamate **10a** (0.591 g, 3.69 mmol) and phenol (2.1 g, 22.3 mmol); yield: 0.678 g (71%); brown solid. Mp: 71-73 °C. IR (neat): 3346, 2925, 1682, 1585, 1534, 1161 cm^{-1}. ^1H NMR (250 MHz, MeOD) δ 8.00 (d, *J* = 8.3 Hz, 1H), 7.82 (d, *J* = 8.3 Hz, 1H), 7.77 – 7.59 (m, 4H), 7.44 – 7.32 (m, 4H), 7.25 (d, *J* = 16.5 Hz, 1H), 7.03 (s, 1H), 3.53 (t, *J* = 5.8 Hz, 2H), 3.42 (t, *J* = 5.8 Hz, 2H), 1.44 (s, 9H) ppm.

^{13}C NMR (63 MHz, MeOD) δ 159.6, 157.6, 153.6, 148.3, 138.3, 136.7, 131.6, 130.3 (3 C), 129.0, 128.7 (2 C), 128.1, 126.1, 122.6, 119.9, 96.6, 80.7, 45.1, 40.4, 29.2 (3c) ppm. Elemental analysis (%) calcd for $C_{24}H_{27}N_3O_2$: C 74.01, H 6.99, N 10.79; found: C 73.85, H 6.84, N 10.46.

***tert*-Butyl (*E*)-(4-((2-styrylquinolin-4-yl)amino)butyl) carbamate (11b).** Prepared from *(E)*-4-chloro-2-styrylquinoline **6** (0.6 g, 2.25 mmol),*tert*-butyl (4-aminobutyl) carbamate **10b** (0.637 g, 3.38 mmol) and phenol (1.91 g, 20.3 mmol); yield: 0.627 g (74%); orange solid. Mp: 93- 95 °C. IR (neat): 3338, 2923, 1681, 1586, 1535, 1162 cm^{-1}. ^{1}H NMR (250 MHz, MeOD) δ 8.07 (d, *J* = 8.4 Hz, 1H), 7.84 (d, *J* = 8.4 Hz, 1H), 7.69 – 7.57 (m, 4H), 7.45 – 7.24 (m, 5H), 6.84 (s, 1H), 3.48 (t, *J* = 6.7 Hz, 2H), 3.14 (t, *J* = 6.7 Hz, 2H), 1.87 – 1.74 (m, 2H), 1.72 – 1.59 (m, 2H), 1.41 (s, 9H) ppm. ^{13}C NMR (63 MHz, MeOD) δ 159.1, 158.2, 153.1, 149.6, 138.5, 135.5, 131.1, 130.3, 130.3 (2 C), 130.0, 129.0, 128.6 (2C), 125.7, 122.5, 120.2, 96.9, 80.3, 44.1, 41.5, 29.2 (3C), 27.2 ppm. Elemental analysis (%) calcd for $C_{26}H_{31}N_3O_2$: C 74.79, H 7.48, N 10.06; found: C 74.54, H 7.51, N 9.70.

General procedure for the synthesis of deprotected polyamino styrylquinolines (12)

The suitable styrylquinoline **11** was dissolved in a mixture of metanol: trifluoroacetic acid (2:1, v/v) and stirred at room temperature for 1h. Once the reaction was finished, the reaction mixture was basified with aqueous NaOH (5 M) and extracted with a mixture of CH_2Cl_2: MeOH (10:1, v/v), which was dried with anhydrous Na_2SO_4 and evaporated *in vacuo* to give the pure product.

***(E)*-N^1-(2-Styrylquinolin-4-yl)ethane-1,2-diamine (12a).** Prepared from compound **11a** (0.578 g, 1.49 mmol); yield: 0.374 g (87%); yellow solid. Mp: 85-86 °C. IR (neat): 3250, 2921, 1583, 1531, 753 cm^{-1}. ^{1}H NMR (250 MHz, MeOD) δ

8.06 (d, *J* = 8.3 Hz, 1H), 7.84 (d, *J* = 8.3 Hz, 1H), 7.68 – 7.55 (m, 4H), 7.43 – 7.22 (m, 5H), 6.87 (s, 1H), 3.51 (t, *J* = 6.3 Hz, 2H), 3.01 (t, *J* = 6.3 Hz, 2H) ppm. ^{13}C NMR (63 MHz, MeOD) δ 158.2, 153.1, 149.5, 138.5, 135.6, 131.2, 130.3 (3 C), 130.1, 129.1, 128.6 (2 C), 125.9, 122.5, 120.3, 96.9, 46.7, 41.5 ppm. Elemental analysis (%) calcd for $C_{19}H_{19}N_3$: C 78.86, H 6.62, N 14.52; found: C 78.56, H 6.72, N 14.32.

***(E)*-N^1-(2-Styrylquinolin-4-yl)butane-1,4-diamine (12b).**

Method A. Prepared from compound **11b** (0.150 g, 0.359 mmol) according to the general procedure described above; yield: 0.100 g (88%); yellow solid. Mp: 68-69 °C. IR (neat): 3261, 2918, 2850, 1580, 1531, 752 cm^{-1}. ^{1}H NMR (250 MHz, MeOD) δ 8.05 (d, *J* = 8.3 Hz, 1H), 7.83 (d, *J* = 8.3 Hz, 1H), 7.68 – 7.53 (m, 4H), 7.44 – 7.22 (m, 5H), 6.78 (s, 1H), 3.41 (t, *J* = 6.7 Hz, 2H), 2.70 (t, *J* = 6.7 Hz, 2H), 1.78 (dd, *J* = 13.8, 6.9 Hz, 2H), 1.64 (dd, *J* = 13.8, 6.9 Hz, 2H) ppm. ^{13}C NMR (63 MHz, MeOD) δ 158.2, 153.1, 149.6, 138.5, 135.5, 131.1, 130.4, 130.3 (2 C), 130.0, 129.1, 128.6 (2C), 125.8, 122.5, 120.2, 96.9, 44.2, 42.6, 31.5, 27.4 ppm. Elemental analysis (%) calcd for $C_{21}H_{23}N_3$: C 79.46, H 7.30, N 13.24; found: C, 79.12; H, 6.93; N, 13.13.

Method B. Ethylenediamine (1.130 g, 18.8 mmol) was added to 4-chloro-2-styrylquinoline **6** (0.250 g, 0.94 mmol) in a pressure-tight microwave tube containing a stirring bar. The mixture was heated under microwave irradiation for 1 h at 120 °C, with an irradiation power of 200 W, using a CEM Discover SP microwave reactor. Thereafter, the cooled reaction mixture was treated with 10% KOH aqueous solution, extracted with CH_2Cl_2, dried with anhydrous Na_2SO_4 and evaporated *in vacuo.* The excess of ethylenediamine was removed by distillation in the presence of EtOH. The resulting residue was subsequently crystallized in Methanol and hexane to give compound **12b** as a yellow solid 0.109 g (40%).

***(E)*-2-Bromo-N-(4-((2-styrylquinolin-4-yl)amino)butyl)acetamide (13a)**. A solution of 2-bromoacetyl bromide (1 eq, 0.53 mmol) in CH_2Cl_2 (20 ml) was slowly added (30 min) using a syringe pump to a solution of compound **12a** (0.170 g, 0.53 mmol) in dichlorometane (20 ml). Once the addition was finished, the reaction mixture was stirred at -5 °C for an additional 30 min period. Then, the resulting crude was basified with an aqueous solution of NaOH (1M) and extracted with a mixture of CH_2Cl_2: MeOH (10:1, v/v), dried with anhydrous Na_2SO_4 and evaporated *in vacuo,* to give the desired product, which was used in the next step without further purification.

The same procedure was used to obtain **(*E*)-2-bromo-N-(2-((2-styrylquinolin-4-yl)amino)ethyl)acetamide (13b)** starting from **12b**.

General procedure for the synthesis of 4-aminostyrylquinolines 14 and 15.

Aliphatic amine derivatives 14.

Compound **13** (80 mg, 0.195 mmol), the suitable amine (1 eq) and Cs_2CO_3 (0.127 g, 0.39 mmol, 2 eq) were suspended in EtOH (1 ml) in a pressure-tight microwave tube containing a stirring bar. The mixture was heated under microwave irradiation for 30 minutes at 120 °C, with an irradiation power of 200 W, using a focused microwave reactor. Thereafter, the cooled reaction mixture was dissolved in CH_2Cl_2 and washed with water, which was re-extracted with CH_2Cl_2. The combined organic layers were dried with anhydrous Na_2SO_4 and evaporated *in vacuo.* The resulting crude products were subsequently crystallized from MeOH-hexane mixtures or purified *via* a neutral alumina column.

(*E*)-2-(Dimethylamino)-N-[2-(2-styrylquinolin-4-ylamino)ethyl]acetamide (14a). Prepared from **13a** (80 mg, 0.195 mmol) and dimethylamine (0.02 ml,

0.195 mmol); the compound was crystallized from a MeOH-hexane mixture to give **14a** (0.052 g, 72%) as an orange powder. Mp 57- 60 °C. IR (neat): 3346, 2923, 2850, 2780, 1660, 1588, 1365, 1044 cm^{-1}. ^1H NMR (250 MHz, $CDCl_3$) δ 7.99 (d, *J* = 8.4 Hz, 1H), 7.85 (d, *J* = 8.4 Hz, 1H), 7.76 (t, *J* = 6.7 Hz, 1H), 7.71 – 7.60 (m, 4H), 7.47-7.32 (m, 5H), 6.62 (s, 1H), 6.55 (br s, 1H), 3.86-3.75 (m, 2H), 3.60 – 3.47 (m, 2H), 3.03 (s, 2H), 2.30 (s, 6H) ppm. ^{13}C NMR (63 MHz, $CDCl_3$) δ 174.0, 156.7, 150.7, 137.3, 133.7, 133.5, 130.5, 129.8 (2C), 129.1 (2C), 128.7, 127.6 (2C), 125.0, 120.6, 118.7, 96.3, 63.3, 46.5 (2C), 46.2, 38.9 ppm. Elemental analysis (%) calcd for $C_{23}H_{26}N_4O$: C 73.77, H 7.00, N 14.96; found: C 73.61, H 7.16, N 14.40.

(*E*)-2-(Diethylamino)-*N*-[2-(2-styrylquinolin-4-ylamino)ethyl]acetamide (14b). Prepared from **13a** (80 mg, 0.195 mmol) and diethylamine (14 mg, 0.195 mmol); the compound was crystallized from a MeOH-hexane mixture to give **14b** (0.056 g, 71 %) as an orange powder. Mp 54- 57 °C. IR (neat): 3341, 2959, 2905, 2850, 1658, 1588, 1430, 1367, 756 cm^{-1}. ^1H NMR (250 MHz, $CDCl_3$) δ 7.99 (d, *J* = 8.4 Hz, 1H), 7.86 (d, *J* = 7.6 Hz, 1H), 7.71-7.59 (m, 4H), 7.49 – 7.30 (m, 5H), 6.62 (s, 1H), 3.85 – 3.75 (m, 2H), 3.60 – 3.46 (m, 2H), 3.12 (s, 2H), 2.56 (q, *J* = 7.1 Hz, 4H), 1.04 – 0.93 (t, *J* = 7.1 Hz, 6H) ppm. ^{13}C NMR (63 MHz, $CDCl_3$) δ 175.6, 156.6, 150.8, 137.2, 133.6, 130.3, 130.3, 129.8, 129.6, 129.1 (2C), 128.7, 127.6 (2C), 125.1, 120.6, 118.7, 96.2, 57.8, 49.2 (2C), 46.2, 38.9, 12.7 (2C) ppm. Elemental analysis (%) calcd for $C_{25}H_{30}N_4O$: C 74.59, H 7.51, N 13.92; found: C 74.52, H 7.10, N 13.50.

(*E*)-2-(pyrrolidin-1-yl)-*N*-(2-(2-styrylquinolin-4-ylamino)ethyl)acetamide (14c). Prepared from **13a** (80 mg, 0.195 mmol) and pyrrolidine (14 mg, 0.195 mmol); the compound was crystallized from a MeOH-hexane mixture to give **14c** (0.054 g, 69 %) as a red solid. Mp 68- 71 °C. IR (neat): 3346, 2918, 2848, 2809, 1655, 1588, 1539, 1365 cm^{-1}. ^1H NMR (250 MHz, $CDCl_3$) δ 7.98 (d, *J* = 7.7 Hz, 1H),

7.85 (d, *J* = 8.1 Hz, 1H), 7.70 – 7.60 (m, 4H), 7.48-7.32 (m, 5H), 6.62 (s, 1H), 6.59 (br s, 1H), 3.85-3-78 (m, 2H), 3.60 – 3.46 (m, 2H), 3.26 (s, 2H), 2.67-2.53 (m, 4H), 1.85-1.75 (m, 4H) ppm. ^{13}C NMR (63 MHz, $CDCl_3$) δ 174.4, 156.7, 150.7, 148.9, 137.3, 133.5, 130.5, 129.8 (2C), 129.1 (2C), 128.7, 127.6 (2C), 125.0, 120.6, 118.7, 96.3, 59.4, 55.1 (2C), 46.2, 38.9, 24.4 (2C) ppm. Elemental analysis (%) calcd for $C_{25}H_{28}N_4O$: C 74.97, H 7.05, N 13.99; found: C 74.04, H 6.98, N 13.83.

(*E*)-2-(Piperidin-1-yl)-*N*-(2-(2-styrylquinolin-4-ylamino)ethyl)acetamide (14d). Prepared from **13a** (80 mg, 0.195 mmol) and piperidine (17 mg, 0.195 mmol); the compound was crystallized from a MeOH-hexane mixture to give **14d** (0.057 g, 70 %) as a yellow solid. Mp 71- 74 °C. IR (neat): 3348, 2936, 2851, 1659, 1563, 1538, 1366, 1129 cm^{-1}. ^{1}H NMR (250 MHz, $CDCl_3$) δ 8.10 (d, *J* = 8.2 Hz, 1H), 7.97 (d, *J* = 8.2 Hz, 1H), 7.8-7.72 (m, 4H), 7.6-7.4 (m, 5H), 6.74 (s, 1H), 3.99 – 3.84 (m, 2H), 3.72-3.58 (m, 2H), 3.14 (s, 2H), 2.62-2.48 (m, 4H), 1.70 – 1.67 (m, 4H), 1.57 – 1.55 (m, 2H) ppm. ^{13}C NMR (63 MHz, $CDCl_3$) δ 174.2, 156.6, 150.8, 137.2, 133.6, 130.3 (2C), 129.8, 129.7, 129.1 (2C), 128.7, 127.6 (2C), 125.1, 120.6, 118.7, 96.2, 62.6, 55.4 (2C), 46.2, 38.9, 26.6 (2C), 24.0 ppm. Elemental analysis (%) calcd for $C_{26}H_{30}N_4O$: C 75.33, H 7.29, N 13.52; found: C 75.66, H 7.05, N 13.70.

(*E*)-2-Morpholino-*N*-[2-(2-styrylquinolin-4-ylamino)ethyl]acetamide (14e). Prepared from **13a** (80 mg, 0.195 mmol) and morpholine (17 mg, 0.195 mmol); the compound was crystallized from a MeOH-hexane mixture to give **14e** (0.048 g, 59%) as an orange powder. Mp 67- 70 °C. IR (neat): 3297, 2918, 2850, 1656, 1599, 1560, 1538, 1464 cm^{-1}. ^{1}H NMR (250 MHz, $CDCl_3$) δ 8.03 (d, *J* = 8.0 Hz, 1H), 7.88 (d, *J* = 8.5 Hz, 1H), 7.79 (br s, 1H), 7.72 -7.57 (m, 4H), 7.48 – 7.31 (m, 5H), 6.59 (s, 1H), 3.88 3.77 (m, 2H), 3.77 – 3.65 (m, 4H), 3.62 – 3.45 (m, 2H), 3.10 (s, 2H), 2.60 – 2.49 (m, 4H) ppm. ^{13}C NMR (63 MHz, $CDCl_3$) δ 173.2, 153.1, 151.5, 147.6, 136.8, 131.4,

130.4, 129.6, 129.2 (2C), 129.1, 128,4, 127.8 (2C), 125.4, 120.9, 118.3, 95.8, 67.3 (2C), 62.2, 54.3 (2C), 45.9, 38.8 ppm. Elemental analysis (%) calcd for $C_{25}H_{28}N_4O_2$: C 72.09, H 6.78, N 13.45; found: C 71.73, H 6.81, N 13.24.

(*E*)-2-(4-Methylpiperazin-1-yl)-*N*-[2-(2-styrylquinolin-4-ylamino)ethyl] acetamide (14f). Prepared from **13a** (80 mg, 0.195 mmol) and 1-methylpiperazine (20 mg, 0.195 mmol); the compound was crystallized from a MeOH-hexane mixture to give **14f** (0.049 g, 59%) as an orange powder. Mp 64- 67 °C. IR (neat): 3348, 2923, 2850, 1666, 1588, 1537, 1373, 756 cm^{-1}. ^1H NMR (250 MHz, $CDCl_3$) δ 7.99 (d, *J* = 8.5 Hz, 1H), 7.83 (d, *J* = 8.1 Hz, 1H), 7.61 – 7.50 (m, 4H), 7.38 – 7.20 (m, 5H), 6.52 (s, 1H), 6.05 (br s, 1H), 3.75 – 3.64 (m, 2H), 3.48 – 3.38 (m, 2H), 3.11 (s, 2H), 2.52 –.2.41 (m, 4H), 2.37 – 2.25 (m, 4H), 2.28 (s, 3H) ppm. ^{13}C NMR (63 MHz, $CDCl_3$) δ 173.5, 156.7, 150.7, 148.9, 137.2, 133.5, 130.4, 129.8 (2C), 129.3 (2C), 128.7, 127.6 (2C), 125.1, 120.5, 118.7, 96.3, 61.6, 55.5 (2C), 53.9 (2C), 46.4, 46.0, 38.9 ppm. Elemental analysis (%) calcd for $C_{26}H_{31}N_5O$: C 72.70, H 7.27, N 16.30; found: C 71.87, H 7.86, N 15.39.

(*E*)-2-(4-Phenylpiperazin-1-yl)-N-[2-(2-styrylquinolin-4-ylamino)ethyl]acetamide (14g). Prepared from **13a** (80 mg, 0.195 mmol) and 1-phenylpiperazine (32 mg, 0.195 mmol); the compound was purified by chromatography through a neutral alumina column using CH_2Cl_2-MeOH (95:5, v/v) as mobile phase to give **14g** (0.043 g, 45%) as an orange solid. Mp: 92- 95 °C. IR (neat): 3352, 2940, 2825, 1661, 1588, 1538, 1435, 969, 757 cm^{-1}. ^1H NMR (250 MHz, MeOD) δ 8.04 (dd, *J* = 8.4, 0.8 Hz, 1H), 7.88 (dd, *J* = 8.4, 0.8 Hz, 1H), 7.76 – 7.61 (m, 4H), 7.47 – 7.31 (m, 5H), 7.23 – 7.15 (m, 2H), 7.03 (s, 1H), 6.86 – 6.78 (m, 3H), 3.68 (s, 2H), 3.35 – 3.31 (m, 4H), 3.03 – 2.97 (m, 2H), 2.59 – 2.52 (m, 2H) ppm. ^{13}C NMR (63 MHz, MeOD) δ 174.2, 158.3, 153.2, 153.0, 149.6, 138.5, 135.9, 131.3,

130.4 (2C), 130.3 (2C), 130.2, 130.1, 129.2, 128.7 (2C), 126.0, 122.4, 121.5, 120.1, 117.9 (2C), 96.8, 62.7, 54.8 (2C), 50.9 (2C), 43.9, 39.7 ppm. Elemental analysis (%) calcd for $C_{31}H_{33}N_5O$: C 75.73, H 6.77, N 14.25; found: C 75.01, H 6.44, N 13.92.

(*E*)-2-(Pyrrolidin-1-yl)-N-[4-((2-styrylquinolin-4-yl)amino)butyl]acetamide (14h)

Prepared from **13b** (80 mg, 0.18 mmol) and pyrrolidine; the crude product was purified by flash chromatography through a silica gel column using hexane: ethyl acetate (3:7, v/v) as the mobile phase to give **14h** as a red solid (0.04 g, 52%). Mp 72-73 °C. IR (neat): 3313, 2922, 2853, 1654, 1582, 1530, 965,754 cm^{-1}. ^1H NMR (250 MHz, MeOD) δ 8.07 (d, *J* = 8.4 Hz, 1H), 7.85 (d, *J* = 8.4 Hz, 1H), 7.71 – 7.57 (m, 4H), 7.46 – 7.24 (m, 5H), 6.82 (s, 1H), 3.48 (t, *J* = 6.6 Hz, 2H), 3.39 – 3.29 (m, 2H), 3.12 (s, 2H), 2.54 (m, 4H), 1.90 – 1.64 (m, 8H) ppm. ^{13}C NMR (63 MHz, MeOD) δ 173.2, 157.5, 152.7, 148.8, 138.0, 135.3, 130.8, 129.9 (2 C), 129.7, 128.4, 128.2 (2 C), 125.4, 122.1, 119.8, 96.5, 59.9, 55.2 (2C), 43.5, 39.7, 28.3, 26.7, 24.6 (2C) ppm. Elemental analysis (%) calcd for $C_{27}H_{32}N_4O$: C 75.67, H 7.53, N 13.07; found: C 74.91, H 7.79, N 12.77.

Ethoxy derivatives (15).

The suitable halide **13** (1 eq) and Cs_2CO_3 (2 eq) were suspended in EtOH (1 ml) in a pressure-tight microwave tube containing a stirring bar. The mixture was heated under microwave irradiation for 30 minutes at 120 °C, with an irradiation power of 200 W, using a focused microwave reactor. Thereafter, the reaction mixture was dissolved in CH_2Cl_2 and washed with water. The combined organic layers were dried with anhydrous Na_2SO_4 and evaporated *in vacuo.* The crude product was

directly purified by flash chromatography through a silica gel column using hexane: ethyl acetate (1:1, v/v) as the mobile phase to give the desire product.

(*E*)-2-Ethoxy-N-(2-((2-styrylquinolin-4-yl)amino)ethyl)acetamide (15a). Prepared from **13a** (0.124 g, 0.3 mmol), and Cs_2CO_3 (0.195 g, 0.6 mmol, 2 eq); yield: 45%, 0.051 g; yellow solid. Mp 59- 61 ºC. IR (neat): 3329, 2865, 2108, 1654, 1583, 1528, 1111,753 cm^{-1}. ^1H NMR (250 MHz, MeOD) δ 7.86 (dd, *J* = 8.4, 0.8 Hz, 1H), 7.73 (dd, *J* = 8.4, 0.8 Hz, 1H), 7.61 – 7.47 (m, 4H), 7.34 – 7.12 (m, 5H), 6.86 (s, 1H), 3.83 (s, 2H), 3.45 (m, 6H), 1.06 (t, *J* = 7.0 Hz, 3H) ppm. ^{13}C NMR (63 MHz, MeOD) δ 173.9, 157.8, 152.6, 149.0, 138.0, 135.5, 130.8, 129.8 (2C), 129.7, 129.6, 129.6, 128.2 (2C), 125.5, 121.9, 119.7, 96.3, 70.7, 68.1, 43.28, 38.9, 15.3 ppm. Elemental analysis (%) calcd for $C_{23}H_{25}N_3O_2$: C 73.57, H 6.71, N 11.19; found: C 73.16, H 6.84, N 10.95.

(*E*)-2-Ethoxy-N-(4-((2-styrylquinolin-4-yl)amino)butyl)acetamide (15b). Prepared from **13b** (0.089 g, 0.2 mmol), and Cs_2CO_3 (0.132 g, 0.40 mmol, 2 eq; yield: 51%, 0.044 g; yellow solid. Mp 52- 54 ºC. IR (neat): 3313, 2925, 2358, 1662, 1585, 1535 cm^{-1}. ^1H NMR (250 MHz, MeOD) δ 8.09 (dd, *J* = 8.4, 0.9 Hz, 1H), 7.86 (dd, *J* = 8.4, 0.9 Hz, 1H), 7.71 – 7.58 (m, 4H), 7.46 – 7.27 (m, 5H), 6.85 (s, 1H), 3.91 (s, 2H), 3.60 – 3.45 (m, 4H), 3.39 – 3.35 (m, 2H), 1.92 – 1.62 (m, 4H), 1.20 (t, *J* = 7.0 Hz, 3H) ppm. ^{13}C NMR (126 MHz, $CDCl_3$) δ 170.6, 156.8, 150.4, 148.9, 137.2, 133.7, 130.3, 130.1, 129.7, 129.1 (2C), 128.7, 127.6 (2C), 124.8, 119.8, 118.7, 97.3, 70.3, 67.5, 43.5, 38.7, 28.2, 26.3, 15.5 ppm. Elemental analysis (%) calcd for $C_{25}H_{29}N_3O_2$: C 74.41, H 7.24, N 10.41; found: C 73.98, H 7.05, N 10.06.

General procedure for the synthesis of glycine derivatives

The suitable aniline (1 eq, 20 mmol) and ethyl 2-bromoacetate (1 eq) were dissolved in dry DMF (100 ml) under argon atmosphere. To this mixture was added NaH (1 eq) portionwise and the reaction was stirred at room temperature for 18 h. Upon completion of the reaction, the solvent was removed under reduced pressure and the residue was suspended in a LiCl aqueous saturated solution (100 ml) and extracted with ethyl acetate (3 x 100 ml) to eliminate the DMF. The combined organic layers were dried with anhydrous Na_2SO_4 and evaporated *in vacuo.* The crude ester thus obtained was hydrolysed using a 5 M aqueous solution of NaOH (2.5 eq) in EtOH (5 ml) at reflux for 1 h. The cooled reaction mixture was extracted with ethyl acetate. The aqueous phase was acidified and extracted again with ethyl acetate, the organic phase was dried with anhydrous Na_2SO_4 and evaporated *in vacuo* to obtain the desired product, which was finally purified by flash chromatography through a silica column using hexane: ethyl acetate as the mobile phase.

***N*-Phenylglycine (16a)**

Prepared from aniline (1.862 g, 20 mmol), and ethyl 2-bromoacetate (3.36 ml, 20 mmol); yield: 51 %, 1.529 g; pale brown solid. Mp 118-120 °C (Lit,[42] 121.8 °C). IR (neat): 3019, 2944, 1556, 1489, 1378, 1314, 692 cm^{-1}. ^1H NMR (250 MHz, MeOD) δ 7.18 – 7.08 (m, 2H), 6.73 – 6.59 (m, 3H), 3.88 (s, 2H) ppm. ^{13}C NMR (63 MHz, MeOD) δ 174.1, 148.3, 129.1 (2C), 117.7, 113.1 (2C), 45.4 ppm. These data are in good agreement with the literature.[54]

***N*-(2,4-Dichlorophenyl)glycine (16b)**

Prepared from 2,4-dichloroaniline (3.220 g, 20 mmol), and ethyl 2-bromoacetate (3.36 ml, 20 mmol); yield: 16 %, 0.704 g; brown solid. Mp 147- 150 °C (Lit,[55] 148-151 °C). IR (neat): 3405, 2875, 2082, 1717, 1593, 1494, 1236, 861, 796 cm^{-1}. ^1H

NMR (250 MHz, MeOD) δ 7.28 (d, *J* = 2.4 Hz, 1H), 7.13 (dd, *J* = 8.7, 2.4 Hz, 1H), 6.57 (d, *J* = 8.7 Hz, 1H), 3.97 (s, 2H) ppm. ^{13}C NMR (63 MHz, MeOD) δ 174.4, 144.4, 130.0, 129.2, 122.8, 120.9, 113.6, 46.1 ppm. Elemental analysis (%) calcd for $C_8H_7Cl_2NO_2$: C 43.67, H 3.21, N 6.37; found: C 43.58, H 3.43, N 6.26.

General procedure for the synthesis of arylamino derivatives.

To a solution of the suitable glycine derivative, 1-ethyl-3-(3-dimethylaminopropyl)carbodiimide hydrochloride (EDC·HCl, 1 eq), and the suitable 2-styrylquinoline derivative **12** (1 eq) in dry THF, Et_3N (2 eq) was added, followed by the addition of 1-hydroxy-7-azabenzotriazole (HOAt, 0.6M solution in DMF, 1 eq). The reaction mixture was refluxed for 12 hours. Then, the solvent was removed under reduced pressure and the residue was suspended in a LiCl saturated aqueous solution (5 ml) and extracted with ethyl acetate (3 × 5 ml). The combined organic layers were dried with anhydrous Na_2SO_4 and evaporated *in vacuo.* The product was purified by flash chromatography through a silica column using hexane: ethyl acetate (1:1, v/v) as the mobile phase to give the desired products.

(*E*)-2-(phenylamino)-N-(2-((2-styrylquinolin-4-yl)amino)ethyl)acetamide (14i)

Prepared from compounds **16a** (0.037 g, 0.127 mmol), and **12a** (0.024 g, 0.127 mmol); yield: 0.018 g (34 %), as a yellow solid. Mp 174- 176 °C. IR (neat): 3362, 2922, 2430, 1657, 1586, 1306, 963, 749, 689 cm^{-1}. ^{1}H NMR (250 MHz, MeOD) δ 7.95 – 7.82 (m, 2H), 7.75 – 7.62 (m, 4H), 7.47 – 7.26 (m, 5H), 7.06 – 6.94 (m, 3H), 6.64 – 6.50 (m, 3H), 3.78 (s, 2H), 3.61 (m, 4H) ppm. ^{13}C NMR (63 MHz, MeOD) δ

175.9, 158.1, 153.2, 149.8, 149.1, 138.5, 136.1, 131.3, 130.5 (2 C), 130.3 (2C), 130.1, 129.8, 128.7, 128.7 (2C), 126.1, 122.4, 120.0, 119.4, 114.2 (2C), 96.7, 49.7, 44.3, 39.5 ppm. HRMS: found m/z 422.2155 [M^+], calculated for $C_{27}H_{26}N_4O$ 422.2107.

(*E*)-2-(Phenylamino)-N-(4-((2-styrylquinolin-4-yl)amino)butyl)acetamide (14j)

Prepared from phenylglycine **16a** (0.042 g, 0.22 mmol), and **12b** (0.070, 0.22 mmol); yield: 26 %, 0.026 g; yellow solid. Mp 82- 85 °C. IR (neat): 3315, 2929, 1654, 1582, 964, 749, 691 cm^{-1}. ^1H NMR (250 MHz, MeOD) δ 8.07 (d, *J* = 7.8 Hz, 1H), 7.87 (d, *J* = 7.8 Hz, 1H), 7.72 – 7.62 (m, 4H), 7.46 – 7.27 (m, 5H), 7.14 – 7.02 (m, 2H), 6.84 (s, 1H), 6.66 – 6.52 (m, 3H), 3.74 (s, 2H), 3.47 (t, *J* = 6.7 Hz, 2H), 3.37 (m, 2H), 1.82 – 1.61 (m, 4H) ppm. ^{13}C NMR (63 MHz, MeOD) δ 174.7, 158.2, 153.1, 149.7, 149.5, 138.5, 135.6, 131.1, 130.5 (2C), 130.3 (3C), 130.1, 129.0, 128.6 (2C), 125.8, 122.5, 120.2, 119.5, 114.3 (2C), 96.9, 49.5, 43.9, 40.2, 28.6, 27.1 ppm. HRMS: found m/z 451.2497 [M+1], calculated for $C_{29}H_{31}N_4O$ 450.2498.

(*E*)-2-((2,4-Dichlorophenyl)amino)-N-(2-((2-styrylquinolin-4-yl)amino)ethyl)acetamide (14k)

Prepared from (2,4-dichlorophenyl)glycine **16b** (0.101 g, 0.46 mmol), and **12a** (0.134 g, 0.46 mmol); yield: 50 %,0.111 g ; yellow solid. Mp 99- 102 °C. IR (neat): 3332, 2922, 1657, 1585, 1500, 754 cm^{-1}. ^1H NMR (250 MHz, MeOD) δ 7.90 (d, *J* = 8.4 Hz, 1H), 7.85 (d, *J* = 8.4 Hz, 1H), 7.73 – 7.60 (m, 4H), 7.45 – 7.19 (m, 6H), 6.96 (s, 1H), 6.80 (dd, *J* = 8.8, 2.4 Hz, 1H), 6.36 (d, *J* = 8.8 Hz, 1H), 3.85 (s, 2H), 3.66 – 3.50 (m, 4H) ppm. ^{13}C NMR (63 MHz, MeOD) δ 173.9, 157.4, 152.9, 148.2, 143.9, 137.9, 136.0, 131.1, 129.9 (2C), 129.8, 129.7, 128.9, 128.7, 128.3 (2C), 128.0, 125.7, 122.9,

122.0, 120.7, 119.5, 113.0, 96.2, 48.2, 43.8, 39.2 ppm. HRMS: found m/z 491.1410 [M+1], calculated for $C_{27}H_{25}Cl_2N_4O$ 491.1405

(*E*)-2-((2,4-Dichlorophenyl)amino)-N-(4-((2-styrylquinolin-4-yl)amino)butyl)acetamide (14l)

Prepared from (2,4-dichlorophenyl)glycine **16b** (0.138 g, 0.63 mmol), and **12b** (0.200 g, 0.63 mmol); yield: 67 %, 0.220 g ; yellow solid. Mp 74- 76 °C. IR (neat): 2929, 2493, 1654, 1581, 1491, 1438, 755 cm^{-1}. ^1H NMR (250 MHz, MeOD) δ 8.04 (d, *J* = 8.4 Hz, 1H), 7.83 (d, *J* = 8.4 Hz, 1H), 7.66 – 7.57 (m, 4H), 7.43 – 7.21 (m, 6H), 7.00 (dd, *J* = 8.7, 2.4 Hz, 1H), 6.80 (s, 1H), 6.44 (d, *J* = 8.7 Hz, 1H), 3.80 (s, 2H), 3.45-3.40 (m, 2H), 3.33-3.29 (m, 2H), 1.75 – 1.67 (m, 4H) ppm. ^{13}C NMR (63 MHz, MeOD) δ 173.2, 158.2, 153.1, 149.6, 144.5, 138.5, 135.6, 131.1, 130.3, 130.3 (2C), 130.1, 130.0, 129.2, 129.0, 128.6 (2C), 125.8, 123.3, 122.5, 121.2, 120.2, 113.5, 96.9, 48.6, 43.90, 40.4, 28.6, 27.2 ppm. HRMS: found m/z 519.1713 [M+1], calculated for $C_{29}H_{29}Cl_2N_4O$ 519.1718.

Synthesis of compound 20.

Compound **17** (0.500 g, 3.1 mmol) and $ZnCl_2$ (0.021 g, 0.15 mmol) were suspended in acetic anhydride (3 ml) in a pressure-tight microwave tube containing a stirring bar. The reaction mixture was heated under microwave irradiation for 5 min at 130 °C, with an irradiation power of 250 W, using a CEM Discover SP microwave reactor. Then, benzaldehyde (0.498 g, 4.7 mmol) was added and the mixture was again heated under microwave irradiation for 25 min at 130 °C. The reaction mixture was basified with an aqueous solution of NaOH (5M) and extracted with CH_2Cl_2, dried with anhydrous Na_2SO_4 and evaporated *in vacuo.* The dark purple

residue was purified by flash chromatography through a silica column using hexane: ethyl acetate (4:1, v/v) as the mobile phase to give 0.335 g (33%) of compound **18** as a yellow solid and 0.265 g (30%) of compound **19** as a white solid.

(*E*)-*N*-Acetyl-*N*-(2-styrylquinolin-4-yl)acetamide (18). Mp 130-133 °C. IR (neat): 2652, 2321, 2112, 1718, 1699, 1362, 1217, 754 cm^{-1}. ^{1}H NMR (250 MHz, $CDCl_3$) δ 8.20 (d, *J* = 8.4 Hz, 1H), 7.86 – 7.55 (m, 7H), 7.49 – 7.36 (m, 4H), 2.39 (s, 6H) ppm. ^{13}C NMR (63 MHz, $CDCl_3$) δ 172.8 (2C), 157.3, 150.2, 145.2, 136.5, 136.0, 131.1, 130.5, 129.5, 129.3 (2C), 128.4, 128.3, 127.8 (2C), 125.0, 121.8, 120.1, 27.05 (2C) ppm. Elemental analysis (%) calcd for $C_{21}H_{18}N_2O_2$: C 76.34, H 5.49, N 8.48; found: C 75.83, H 5.47, N 8.25.

(*E*)-*N*-(2-Styrylquinolin-4-yl)acetamide (19). Mp 198- 200 °C. IR (neat): 3258, 2322, 1737, 1657, 1523, 1371, 954, 755 cm^{-1}. ^{1}H NMR (250 MHz, $CDCl_3$) δ 8.31 (s, 1H), 7.86 (d, *J* = 8.4 Hz, 2H), 7.56 (d, *J* = 8.4 Hz, 1H), 7.51 – 7.37 (m, 4H), 7.30 – 7.05 (m, 6H), 2.14 (s, 3H) ppm. ^{13}C NMR (63 MHz, $CDCl_3$) δ 169.3, 156.9, 148.9, 140.5, 136.5, 134.9, 130.3, 129.8, 129.0, 128.9 (2C), 128.8, 127.4 (2C), 126.1, 119.3, 119.1, 109.5, 25.2 ppm. Elemental analysis (%) calcd for $C_{19}H_{16}N_2O$: C 79.14, H 5.59, N 9.72; found: C 78.74, H 5.47, N 9.37.

(*E*)-2-Styrylquinolin-4-amine (20)

Compound **18** (0.150 g, 0.454 mmol) and KOH (5M) (10 eq) were dissolved in MeOH (3 ml) in a pressure tight microwave tube containing a stirring bar. The reaction mixture was heated under microwave irradiation for 1 hour at 135 °C, with an irradiation power of 200 W, using a CEM Discover SP microwave reactor. Thereafter, the reaction mixture was extracted with ethyl acetate, dried with anhydrous Na_2SO_4 and evaporated *in vacuo,* to give compound **20** (0.100 g, 89%

yield) as a yellow solid. Mp 103- 106 °C. IR (neat): 3446, 3296, 3047, 2920, 1640, 1578, 1511, 967, 752 cm^{-1}.^{1}H NMR (250 MHz, $CDCl_3$) δ 8.03 (dd, *J* = 8.5, 0.6 Hz, 1H), 7.75 (d, *J* = 8.5 Hz, 1H), 7.72 – 7.58 (m, 4H), 7.47 – 7.26 (m, 5H), 6.91 (s, 1H), 4.79 (s, 2H) ppm.^{13}C NMR (63 MHz, $CDCl_3$) δ 156.3, 149.9, 149.0, 136.8, 133.7, 129.9, 129.7, 129.4, 128.9 (2C), 128.5, 127.3 (2C), 124.7, 120.2, 118.4, 101.7 ppm. Elemental analysis (%) calcd for $C_{17}H_{14}N_2$: C 82.90, H 7.73, N 11.37; found: C 81.92, H 5.92, N 11.08.

When applied to **19** (0.200 g, 0.69 mmol), the same procedure furnished 0.150 g of compound **20** (88% yield).

General procedure for the synthesis of compounds 21 and 22.

4-Chloro-2-styrylquinoline **6** (0.100 g, 0.34 mmol), the suitable nucleophile and 10% mol of $InCl_3$ (8 mg) were charged in a pressure-tight microwave tube containing 2 mL of acetonitrile and a stirring bar. The reaction mixture was submitted to microwave irradiation for 1 h at 150 °C, with an irradiation power of 150 W, using a CEM Discover focused microwave reactor. The cooled reaction mixture was dissolved in CH_2Cl_2, which was washed with H_2O, dried with anhydrous Na_2SO_4, and evaporated. The pure compounds were obtained by flash chromatography of the evaporation residue.

(*E*)-2-((diethylamino)methyl)-4-(2-styrylquinolin-4-ylamino)phenol (21). Prepared from compound **6** (0.100 g, 0.34 mmol) and 4-amino-α-diethylamino-*o*-cresol (66 mg, 0.34 mmol). The crude reaction product was purified by chromatography through a neutral alumina column using CH_2Cl_2/MeOH (95:5, v/v) as mobile phase to give **21** in 54 % yield (0.078 g). Mp 127-130 °C. IR (neat): 3176, 3050, 3026, 1586, 1552, 1492, 1439, 1257, 752 cm^{-1}. ^{1}H NMR (250 MHz,

MeOD) δ 8.38 (d, *J* = 8.4 Hz, 1H), 7.96 (d, *J* = 8.3 Hz, 1H), 7.86 (t, *J* = 7.7 Hz, 1H), 7.66 – 7.54 (m, 3H), 7.43 - 7.35 (m, 3H), 7.27 – 7.14 (m, 2H), 7.04 (d, *J* = 9.3 Hz, 1H), 6.97 (s, 1H), 6.78 (d, *J* = 8.4 Hz, 2H), 4.17 (s, 2H), 3.03 (q, *J* = 7.1 Hz, 4H), 1.30 (t, *J* = 7.1 Hz, 6H) ppm. ^{13}C NMR (63 MHz, MeOD) δ 158.1, 155.0, 145.2, 138.8, 137.4, 133.7, 131.7, 131.1, 130.5 (2C), 129.3, 129.1 (2C), 128.9, 127.5, 125.5, 125.2, 123.5, 122.6, 120.9, 119.5, 118.4, 99.4, 55.3, 48.6 (2C), 10.8 (2C) ppm. Elemental analysis (%) calcd for $C_{28}H_{29}N_3O$: C 79.40, H 6.90, N 9.92; found: C 78.91, H 6.50, N 9.39.

(*E*)-4-(1*H*-Indol-3-yl)-2-styrylquinoline (22). Prepared from compound **6** (0.100 g, 0.34 mmol) and indole (44 mg, 0.34 mmol). The pure compound **22** was obtained by flash chromatography on silica gel as a pale yellow solid (0.068 g, 58%). Mp 94- 97 ^{o}C. IR (neat): 3408, 3054, 3028, 1586, 1500, 1243, 962, 742 cm^{-1}. ^{1}H NMR (250 MHz, $CDCl_3$) δ 8.79 (br s, 1H), 8.22 (d, *J* = 8.4 Hz, 1H), 8.14 (d, *J* = 8.4 Hz, 1H), 7.82 (d, *J* = 19.5 Hz, 1H), 7.78 – 7.66 (m, 4H), 7.59 – 7.54 (m, 3H), 7.48 – 7.33 (m, 6H), 7.28 – 7.22 (m, 1H) ppm. ^{13}C NMR (63 MHz, $CDCl_3$) δ 156.1, 149.3, 142.8, 137.0, 136.7, 134.8, 130.1, 129.8, 129.5, 129.2 (2C), 129.0, 127.7 (2C), 127.3, 127.2, 126.7, 126.4, 125.0, 123.4, 121.1, 120.5, 120.2, 114.6, 112.1 ppm. Elemental analysis (%) calcd for $C_{25}H_{18}N_2$: C 86.68; H 5.24; N 8.09; found: C 86.53, H 5.44, N 7.76.

Biological studies

General remarks

Assay interference was discarded by the following reasons: (a) There is no structural reason to suspect protein reactivity or singlet-oxygen quenching. (b) Membrane disruption was specifically discarded in one the assays. (c) All assays

involving fluorescence detection were guided by the maxima observed in the fluorescence spectra of the compounds involved. In the fluorescence microscopy and TX-100 membrane permeabilization experiments, controls were used to discard interferences. (d) Controls for luciferase inhibition were also employed.

Cells

Promastigotes from *Leishmania donovani* strain MHOM/SD/00/1S-2D were grown at 26 °C in RPMI 1640-modified medium, supplemented with 10% heat-inactivated fetal calf serum (HIFCS). Promastigotes of 3 Luc, a surrogated strain with episomal expression of a cytoplasmic form of *Photinus pyralys* luciferase, were grown under identical conditions except for the addition of G-418 (30 μg/ml, final concentration) in the growth medium. *L. pifanoi* axenic amastigotes (strain MHOM/VE/60/Ltrod) were maintained in medium 199 (Gibco-BRL) supplemented with 20% HIFCS and 50 μg/ ml hemin at 32 °C.[56]

Cells from the murine macrophage line J774 were provided by the Culture Cell Facility of Centro de Investigaciones Biológicas. Cells were grown in in RPMI 1640-plus 10% (HIFCS) at 37 °C in 5% CO_2.

Peritoneal macrophages were obtained from 8-week-old Balb/C mice prior elicitated by *i.p.* injection of 1 ml 4% sodium thioglycollate three days before extraction. Macrophages were harvested by peritoneal washing with Hanks' buffer supplemented with glucose (HBSS-Glc) (137 mM NaCl, 5.3 mM KCl, 0.4 mM KH_2PO_4, 4.2 mM $NaHCO_3$, 0.4 mM Na_2HPO_4, 10 mM D-glucose, pH 7.2), washed with the same medium, resuspended in RPMI 1640 + 10 % HIFCS. Protocols were approved by the Animal Welfare Committee of Centro de Investigaciones

Biológicas and authorized by the Autonomic Government of Madrid (Permission number: PROEX 070/18).

Leishmanicidal activity on axenic parasites and cellular toxicity of styrylquinolines

Parasites were harvested at late exponential phase of growth phase by centrifugation. Afterwards, they were washed once with HBSS-Glc and resuspended in their corresponding fresh growth medium (2×10^6 cells/ml) containing the compound to be assayed (concentration range: 0.78-50.0 μM). Parasites were allowed to proliferate either for 72 h at 26 °C, or 96 h at 32 °C, for promastigotes or amastigotes, respectively. Proliferation was measured by reduction of MTT (3-(4, 5-dimethylthiazol-2-yl)-2, 5-diphenyltetrazolium bromide) (0.5 mg/ml, 2 h). The resulting formazan was solubilized in SDS (5% w/v, final concentration) and read at 590 nm in a 610 Bio-Rad plate reader. Samples were made by triplicate and experiments were repeated at least twice. IC_{50} (the concentration of the compound that inhibited parasite proliferation by half) was determined using the statistical package of Sigma Plot 12.5 software.

Cells of the tumoral murine macrophage line J774.1 (Cell Culture Facility, April 2018) were grown in RPMI-1640 medium (Gibco) supplemented with 10% heat inactivated foetal calf serum, 2 mM L-glutamine and penicillin-streptomycin at 37ºC, in 5% CO_2. Cells were detached from the plate by trypsinization and seeded in a 96 microwell plate (10^5 cells/well). Cells were allowed to adhere overnight. Next day, the medium was removed and substituted with fresh medium containing the corresponding concentration of drug, and incubated for additional 48 h.

Afterwards, MTT was added (0.5 mg/ml, final concentration) and reduction to formazan allowed to proceed for 2h. Then, SDS (0.1%, final concentration) was added to solubilize the precipitated formazan for 2h at 37ºC. Finally, the plate was read in a 680 Bio-Rad plate Reader with a 595 nm filter. At least two independent experiments were carried out using triplicate samples. CC_{50} was calculated using the statistical package of Sigma Plot vs 12.5.

Peritoneal macrophages were resuspended in RPMI-1640 + 10% HIFCS and aliquoted into a 96 well plate (10^5 cells/well). Next day, cells were washed with HBSS-Glc at 37 °C, incubated with the compounds for 48 h and MTT reduction assayed and read as described above.

Assessment of leishmanicidal activity on *L. pifanoi* intracellular parasites

Peritoneal macrophages resuspended in RPMI-10% HIFCS were seeded into 24 well microplate at 2 × 10^5 cells/well and allowed to attach onto a sterile 14 mm diameter circular glass coverslide placed at the bottom of the well. Cells were allowed to adhere overnight. Next day, macrophages were incubated with *L. pifanoi* amastigotes (cell ratio 4:1) for 4 h. Prior to their addition into macrophage culture, amastigotes were previously labeled with CFSE (carboxyfluorescein succinimidyl ester) as previously described.[42] Non-phagocytosed parasites were eliminated by extensive washing. Infection was allowed to proceed for 24 h. Afterwards, fresh medium containing the different styrylquinolines at 10 μM (final concentration) was added to the cells, and incubated for 12 h. Variation of the parasite load was assessed by confocal microscopy on a Leica TCS-SP2-AOBS-UV ultraspectral confocal microscope (Leica Microsystems, Heidelberg, Germany), by

counting the number of parasites and macrophages in five different fields of each preparation, each containing at least 100 macrophages. At least 4 determinations were carried out for each sample. Cells were labeled with DAPI (5 μg/ml) prior to observation. Fluorescence settings: CFSE (carboxyfluorescein succinimidyl ester) (λ_{exc} = 488 nm/ λ_{em} = 520 nm, green fluorescence); DAPI (λ_{exc} = 350 nm/ λ_{em} = 460 nm, blue fluorescence).

Variation of free cytoplasmic ATP in *L. donovani* promastigotes

Real-time variation of the levels of free cytoplasmic ATP in living parasites, caused by the compounds, was monitored in living *L. donovani* promastigotes (3-Luc strain). These parasites express an episomal cytoplasmic form of *Photinus pyralis* luciferase. Briefly,[57] 3-Luc promastigotes were resuspended in HBSS-Glc at 20 × 10^6 cells/ml, thereafter considered as the standard conditions; the free membrane permeable luciferase substrate DMNEP-D-luciferin (D-luciferin, 1-(4,5-dimethoxy-2-nitrophenylethyl ester) (Gold Biotechnology, St Louis, MO) was added into the suspension (50 μM, final concentration). Parasites were immediately aliquoted (100 μl/well) into a black 96-well microplate. Luminescence variation was monitored in a BMG Polarstar Galaxy microwell reader (Öffenburg, Germany). When luminescence reached a plateau, drugs at different concentrations were added (t = 0) Data were referred as the percentage of luminescence at the addition of the drug (t = 0), considered as 100% luminescence.

Plasma membrane permeabilization of *L. donovani* promastigotes

Permeabilization of the plasma membrane of *L. donovani* promastigotes was measured by the increase of fluorescence of the vital dye Sytox Green (MW = 600) (InVitrogen), once bound into intracellular nucleic acids. Briefly, promastigotes

were prepared under standard conditions, except for the addition of SYTOX Green (1.0 μM, final concentration) into the incubation medium, and dispensed into a black 96 microwell plate (100 μL/well). Once a stable readout was obtained, drug was added. The increase in fluorescence (λ_{exc} = 504 nm/λ_{em} = 524 nm) caused was monitored in a BMG Polarstar Galaxy Microwell Reader (Öffenburg, Germany). Results were expressed as percentage relative to full permeabilized cells, achieved by addition of 0.1% Triton X-100.

Variation of the mitochondrial electrochemical potential $\Delta\Psi_m$) in *L. donovani* promastigotes.

L. donovani promastigotes (prepared under the standard conditions aforementioned) were aliquoted into a 96 microwell plate (100 μL/well) and incubated with the compound under study at different concentrations. Afterwards, rhodamine 123 [2-(6-amino-3-imino-3*H*-xanthen-9-yl) benzoic acid methyl ester, hydrochloride] (Invitrogen) was added (0.3 μg/ml, final concentration). The cells were incubated for 5 min at 37 °C and washed extensively with HBSS-Glc. Finally, the promastigotes were resuspended at 10^6 cells/ml in HBSS-Glc, and analyzed in a FC500 Coulter cytofluorometer. Fluorescence settings for rhodamine 123 were λ_{exc} = 488 nm/ λ_{em} = 525 nm. Untreated parasites, or those with fully depolarized mitochondria (achieved by incubation with 20 mM KCN for 30 min) were considered as positive and negative controls, respectively.

Intracellular distribution of styrylquinoline 15a in *L. pifanoi* axenic amastigotes by confocal microscopy.

Amastigotes under standard conditions were incubated with styrylquinoline **15a** (1h, 32 °C). Immediately prior to observation, cells were additionally stained with

DAPI (2-(4-amidinophenyl)-1H -indole-6-carboxamidine) (5 μg/ml, 30 min, 26 °C). Confocal fluorescence images were obtained in living parasites on a Leica TCS-SP2-AOBS-UV ultraspectral confocal microscope (Leica Microsystems, Heidelberg, Germany). Fluorescence settings were λ_{exc} = 488 nm/λ_{em} = 520 nm for styrylquinolines[58] and λ_{exc} = 350 nm/ λ_{em} = 460 nm for DAPI. Amastigotes with a full by reversible depolarized mitochondrion were obtained by incubation with 1 mM KCN[43] 15 min prior to styrylquinoline addition. The mitochondrial accumulation of styrylquinoline **15a** inside the *Leishmania* mitochondrion was assessed by double labelling of the parasites with **15a**, and Mitotracker Red (Invitrogen) as specific fluorescent marker for this organelle. To this end parasites were first incubated with Mitotracker Red (0.05 μM, 10 min, 32 ºC), then the styrylquinoline derivative was added (15 μM, 1h, 32 ºC). DAPI were used for the intracellular location of intracellular DNA. Fluorescence settings were λ_{exc} = 488 nm/λ_{em} = 520 nm for styrylquinolines,[58] λ_{exc} = 350 nm/ λ_{em} = 460 nm for DAPI; and λ_{exc} = 570 nm/ λ_{em} = 590 nm for Mitotracker Red. Pearson coefficient (r) was calculated using ImageJ1.51d software.[59]

Analysis of DNA content in promastigotes

Promastigotes (4 $\times 10^6$ cells /ml) were incubated with different concentrations of **15a** for 48 h at 26 °C in complete culture medium. Next, parasites were washed twice with HBSS, fixed in ice-cold ethanol overnight at 4 °C, and washed again twice with HBSS. Cells were then resuspended in 500 μL of HBSS containing 20 μg/ml propidium iodide (PI) plus 0.5 mg/ml RNAse and incubated for 30 min at room temperature in the dark. DNA content was analyzed by flow cytometry in an

FC500 Coulter cytofluorometer. Fluorescence settings: λ_{exc} = 488 nm/ λ_{em} = 620 nm.

Transmission electron microscopy

L. donovani promastigotes were incubated in full growth medium 12 h with 5 μM styrylquinoline **15a**, a concentration causing 50% inhibition of MTT reduction in HBSS-Glc under these conditions. Next, they were collected by centrifugation, washed twice with HBSS, fixed in 5% (w/v) glutaraldehyde in the same medium, and included with 2.5% (w/v) OsO_4 for 1 h. Cells were dehydrated in increasing concentrations of ethanol [30, 50, 70, 90, and 100% (v/v); 30 min each], incubated with propylene oxide (1 h), and embedded in increasing concentrations of Epon 812 resin. After polymerization of the resin, samples were cut in a microtome with a diamond knife and observed in a Jeol-1230 electron microscope.[49]

Accumulation of acridine orange in acidocalcisomes of *L. donovani* promastigotes

Promastigotes (40 × 10^6 cells/ml), were loaded with 2 μM of acridine orange (5 min, 26 °C). Afterwards, non-incorporated dye was eliminated by washing and parasite suspension adjusted to the original parasite density. For kinetic accumulation experiments, 100 μL/well of this parasite suspension were dispensed into a black 96 microwell plate. Fluorescence measurements were carried out in a BMG Polarstar Galaxy Microwell Reader (Öffenburg, Germany) (λ_{exc} = 488 nm/ λ_{em} = 530 nm). Once a stable readout was obtained, styrylquinolines were added at 5 μM, and variation in fluorescence monitored. Acidocalcisome alkalinization by styrylquinolines **15a** and **23** was also visualized by confocal microscopy. Cells loaded with acridine orange were prepared as above,

and further incubated with these two styrylquinolines at 5 μM for 1 h. Cells were then washed twice, and confocal fluorescence images were acquired on living promastigotes immobilized on hydrogel Cygel (bioStatus, Leicestershire, UK) on a Leica TCS-SP2-AOBS-UV ultraspectral confocal microscope (Leica Microsystems, Heidelberg, Germany). Fluorescence settings for acridine orange were λ_{exc} = 488 nm/ λ_{em} = 650 nm.

ASSOCIATED CONTENT

Supporting Information

Supplementary data to this article can be found online at xxx.

AUTHOR INFORMATION

Corresponding Authors

* Luis Rivas (luis.rivas@cib.csic.es), Maria Laura Bolognesi (marialaura.bolognesi@unibo.it), J. Carlos Menéndez (josecm@farm.ucm.es).

Author Contributions

The manuscript was written through contributions of all authors. / All authors have given approval to the final version of the manuscript. / ‡These authors contributed equally.

Funding Sources

MIUR; Ministerio de Economía y Competitividad (MINECO); Universidad Complutense, Madrid; CSIC; Instituto de Salud Carlos III, Subdirección General de Redes y Proyectos Cooperativos-FEDER.

ACKNOWLEDGMENT

This research was supported by the following grants; (a) MLB: MIUR, PRIN 201274BNKN_003; (b) JCM: Universidad Complutense (GR3/14) and MINECO (CTQ2015-68380-R); (c) LR: RD16/0027/0010, CSIC PIE-201020E054 and MINECO SAF2015-65740-R. A predoctoral contracts to MS from Universidad Complutense and a FPI contract to MP from MINECO (BES-2016-076410P) are also gratefully acknowledged.

ABBREVIATIONS

AO, acridine orange; CFSE, carboxyfluorescein succinimidyl ester; DNDi, Drugs for Neglected Diseases initiative; MTR, MitoTracker Red; SI, selectivity index.

REFERENCES

1. Alvar, J.; Vélez, I. D.; Bern, C.; Herrero, M.; Desjeux, P.; Cano, J.; Jannin, J.; den Boer, M. Leishmaniasis worldwide and global estimates of its incidence. *PLoS ONE* **2012**, *7*: e35671.
2. Goupil, L. S.; McKerrow. J. H. Introduction: Drug discovery and development for neglected diseases. *Chem. Rev.* **2014**, *114*, 11131-11137.
3. Burza, S., Croft, S. L., Boelaert, M. Leishmaniasis. *Lancet* **2018**, *392*, 951-970.
4. Reguera, R.; Calvo-Álvarez, E.; Álvarez-Velilla, R.; Balaña-Fouce, R. Target-based vs. phenotypic screenings in *Leishmania* drug discovery: A marriage of convenience or a dialogue of the deaf? *Int. J. Parasitol. Drugs Drug Resist.* **2014**, *4*, 355-357.
5. Ponte-Sucre, A.; Gamarro, F., Dujardin, J.C.; Barrett, M. P.; López-Vélez, R; García-Hernández, R.; Pountain, A. W.; Mwenechanya, R.; Papadopoulou, B.

Drug resistance and treatment failure in leishmaniasis: A 21st century challenge. *PLoS Negl. Trop. Dis.* **2017**, *11*:e0006052.

6. Kumar, A.; Pandey, S. C,.; Samant, M. Slow pace of antileishmanial drug development. *Parasitology Open* **2018**, *4*, e4, 1–11. .
7. Mowbray, C.E. Anti-leishmanial Drug Discovery: Past, Present and Future Perspectives in Drug Discovery for Leishmaniasis. 2018 RSC Drug Discovery Series 60, 24-36 (Eds Rivas, L. and Gil, C.) Ed Royal Society of Chemistry, London, UK.
8. Nagle, A. S.; Khare, S.; Kumar, A. B.; Supek, F.; Buchynskyy, A.; Mathison, C. J.; Chennamaneni, N. K.; Pendem, N.; Buckner, F. S.; Gelb, M. H.; Molteni, V. Recent developments in drug discovery for leishmaniasis and human African trypanosomiasis. *Chem. Rev.* **2014**, *114*, 11305-11347.
9. Reynolds, K. A.; Loughlin, W.A.; Young, D. J. Quinolines as chemotherapeutic agents for leishmaniasis. *Mini Rev. Med. Chem.* **2013**, *13*, 730-743.
10. Desrivot, J.; Herrenknecht, C.; Ponchel, G.; Garbi, N.; Prina, E.; Fournet, A.; Bories, C.; Figadère, B.; Hocquemiller, R.; Loiseau, P. M. Antileishmanial 2-substituted quinolines: *In vitro* behaviour towards biological components. *Biomed. Pharmacother.* **2007**, *61*, 441-450.
11. Fakhfakh, M. A.; Fournet, A.; Prina, E.; Mouscadet, J. F.; Franck, X.; Hocquemiller, R.; Figadère, B. Synthesis and biological evaluation of substituted quinolines: potential treatment of protozoal and retroviral co-infections. *Bioorg. Med. Chem.* **2003**, *11*, 5013-5023.
12. Franck, X.; Fournet, A.; Prina, E.; Mahieux, R.; Hocquemiller, R.; Figadère, B. Biological evaluation of substituted quinolines. *Bioorg. Med. Chem. Lett.* **2004**, *14*, 3635-3638.

13. Nakayama, H.; Desrivot, J.; Bories, C.; Franck, X.; Figadère, B.; Hocquemiller, R.; Fournet, A.; Loiseau, P. M. *In vitro* and *in vivo* antileishmanial efficacy of a new nitrilquinoline against *Leishmania donovani*. *Biomed. Pharmacother.* **2007**, *61*, 186-188.

14. Loiseau, P. M.; Gupta, S.; Verma, A.; Srivastava, S.; Puri, S. K.; Sliman, F.; Normand-Bayle, M.; Desmaele, D. *In vitro* activities of new 2-substituted quinolines against *Leishmania donovani*. *Antimicrob. Agents Chemother.* **2011**, *55*, 1777-1780.

15. Stevanović, S.; Perdih, A.; Senćanski, M.; Glišić, S.; Duarte, M.; Tomás, A. M.; Sena, F. V.; Sousa, F. M.; Pereira, M. M.; Solmajer, T. *In silico* discovery of a substituted 6-methoxy-quinalidine with leishmanicidal activity in *Leishmania infantum*. *Molecules* **2018**, *23*:772.

16. Loiseau, P. M.; Cojean, S.; Schrével. J. Sitamaquine as a putative antileishmanial drug candidate: from the mechanism of action to the risk of drug resistance. *Parasite* **2011**, *18*, 115-119.

17. Carvalho, L.; Luque-Ortega, J. R.; López-Martín, C.; Castanys, S.; Rivas, L.; Gamarro, F. The 8-aminoquinoline analogue sitamaquine causes oxidative stress in *Leishmania donovani* promastigotes by targeting succinate dehydrogenase. *Antimicrob. Agents Chemother.* **2011**, *55*, 4204-4210.

18. Carvalho, L.; Luque-Ortega, J. R.; Manzano, J. I.; Castanys, S.; Rivas, L.; Gamarro, F. Tafenoquine, an antiplasmodial 8-aminoquinoline, targets *Leishmania* respiratory complex III and induces apoptosis. *Antimicrob. Agents Chemother*. **2010**, *54*, 5344-5351.

19. Lizzi, F.; Veronesi, G.; Belluti, F.; Bergamini, C.; López-Sánchez, A.; Kaiser, M.; Brun, R.; Krauth-Siegel, R. L.; Hall, D. G.; Rivas, L.; Bolognesi, M. L. Conjugation

of quinones with natural polyamines: Toward an expanded antitrypanosomatid profile. *J. Med. Chem*. **2012**, *55*, 10490-10500.

20. O'Sullivan, M. C.; Durham, T. B.; Valdes, H. E.; Dauer, K. L.; Karney, N. J.; Forrestel, A. C.; Bacchi, C. J.; Baker, J. F. Dibenzosuberyl substituted polyamines and analogs of clomipramine as effective inhibitors of trypanothione reductase; molecular docking, and assessment of trypanocidal activities. *Bioorg. Med. Chem*. **2015**, *23*, 996–1010.
21. Sen, N.; Das, B. B.; Ganguly, A.; Banerjee, B.; Sen, T.; Majumder, H. K. *Leishmania donovani*: intracellular ATP level regulates apoptosis-like death in luteolin induced dyskinetoplastid cells. *Exp. Parasitol.* **2006**, *114*, 204-214.
22. Saunders, E. C.; Ng, W. W.; Kloehn, J.; Chambers, J. M.; Ng, M.; McConville, M. J. Induction of a stringent metabolic response in intracellular stages of *Leishmania mexicana* leads to increased dependence on mitochondrial metabolism. *PLoS Pathogens* **2014**, *10*, art. no. e1003888.
23. Manzano, J. I.; Carvalho, J.; Pérez-Victoria, J. M.; Castanys, S.; Gamarro, F. Increased glycolytic ATP synthesis is associated with tafenoquine resistance in *Leishmania major. Antimicrob. Agents Chemother*. **2011**, 55, 1045–1052
24. Fidalgo, L. M.; Gille, L. Mitochondria and trypanosomatids: targets and drugs. *Pharm Res*. **2011**, *28*, 2758-2770.
25. Murphy, M. P. Targeting lipophilic cations to mitochondria. *Biochim Biophys Acta* **2008**, *1777*, 1028-1031.
26. Antoine, J. C.; Prina, E.; Jouanne, C.; Bongrand, P. Parasitophorous vacuoles of *Leishmania amazonensis*-infected macrophages maintain an acidic pH. *Infect Immun*. **1990**, *58*, 779-787.

27. Dias, M. P.; Souza, I. O.; Lima, W. P.; Gameiro, J.; da Silva, A. D.; Coimbra, E. S. 4-Aminoquinoline derivatives as potential antileishmanial agents. *Chem. Biol. Drug Des*. **2015**, *86*, 704–714.

28. Palit, P.; Hazra, A.; Maity, A.; Vijayan, R. S. K.; Manoharan, P.; Banerjee, S.; Mondal, N. B.; Ghoshal, N.; Ali, N. Discovery of safe and orally effective 4-aminoquinaldine analogues as apoptotic inducers with activity against experimental visceral leishmaniasis. *Antimicrob. Agents Chemother.* **2012**, *56*, 432–445.

29. Guglielmo, S.; Bertinaria, M.; Rolando, B.; Crosetti, M.; Fruttero, R.; Yardley, V.; Croft, S. L.; Gasco, A. A new series of amodiaquine analogues modified in the basic side chain with in vitro antileishmanial and antiplasmodial activity. *Eur. J. Med. Chem*. **2009**, *44*, 5071-5079.

30. Ray, S.; Sadhukhan, P. K.; Mandal, N. B.; Mahato, S. B.; Majumder H. K. Dual inhibition of DNA topoisomerases of *Leishmania donovani* by novel indolyl quinolines. *Biochem. Biophys. Res. Commun*. **1997**, *230*, 171-175.

31. Daina, A; Michielin, O; Zoete, V; SwissADME: a free web tool to evaluate pharmacokinetics, drug-likeness and medicinal chemistry friendliness of small molecules. *Sci. Rep.* **2017,** *7*, 42717.

32. Chang, F.-S.; Chen, W.; Wang, C.; Tzeng, C.-C.; Chen, Y.-L. Synthesis and antiproliferative evaluations of certain 2-phenylvinylquinoline (2-styrylquinoline) and 2-furanylvinyl-quinoline derivatives. *Bioorg*. *Med*. *Chem*. **2010**, *18*, 124–133.

33. Staderini, M.; Bolognesi, M. L.; Menéndez, J. C. Lewis acid–catalyzed generation of C-C and C-N bonds on π-deficient heterocyclic substrates. *Adv. Synth. Catal*. **2015**, *357*, 185-195.

34. Sridharan, V.; Avendaño, C.; Menéndez, J. C. Convenient, two-step synthesis of 2-styrylquinolines: An application of the CAN-catalyzed vinylogous type-II Povarov reaction. *Tetrahedron* **2009**, *65*, 2087–2096.

35. Tielens, A. G.; van Hellemond, J. J. Surprising variety in energy metabolism within *Trypanosomatidae*. *Trends Parasitol.* **2009**, *25*, 482-490.

36. Saugar, J. M.; Delgado, J.; Hornillos, V.; Luque-Ortega, J. R.; Amat-Guerri, F.; Acuna, A. U.; Rivas, L. Synthesis and biological evaluation of fluorescent leishmanicidal analogues of hexadecylphosphocholine (miltefosine) as probes of antiparasite mechanisms. *J. Med. Chem*. **2007**, *50*, 5994-6003.

37. Coimbra, E. S.; Antinarelli, L. M. R.; Silva, N. P.; Souza, I. O.; Meinel, R. S.; Rocha, M. N.; Soares, R. P. P.; da Silva, A. D. Quinoline derivatives: Synthesis, leishmanicidal activity and involvement of mitochondrial oxidative stress as mechanism of action. *Chem.-Biol. Interact.* **2016**, *260*, 50-57.

38. An, A. A.; Duboise, S. M.; Eperon, S.; Rivas, L.; Hodgkinson, V.; Traub-Cseko, Y.; McMahon-Pratt, D. Developmental life cycle of *Leishmania*—Cultivation and characterization of cultured extracellular amastigotes. *J. Eukaryot. Microbiol.* **1993**, *40*, 213-223.

39. Peters, W.; Trotter, E. R.; Robinson, B. L. The experimental chemotherapy of leishmaniasis, VII. Drug responses of *L. major* and *L. mexicana amazonensis*, with an analysis of promising chemical leads to new antileishmanial agents. *Ann. Trop. Med. Parasitol*. **1980**, *74*, 321–335.

40. Yardley, V., Koniordou, M. Drug assay methodology in leishmaniasis: From the microplate to image analysis, in Rivas, L.; Gil, C. Drug discovery for leishmaniasis, RSC Drug Discovery Series, 2018, Chapter 4, pp. 57-76.

41. Luque-Ortega, J. R.; Rivero-Lezcano, O. M.; Croft, S. L.; Rivas, L. *In vivo* monitoring of intracellular ATP levels in *Leishmania donovani* promastigotes as a rapid method to screen drugs targeting bioenergetic metabolism. *Antimicrob. Agents Chemother.* **2001**, *45*, 1121-1125.

42. Luque-Ortega, J. R.; Rivas, L. Characterization of the leishmanicidal activity of antimicrobial peptides. *Methods Mol. Biol.* **2010**, *618*, 393-420.

43. Van Hellemond, J. J.; Tielens, A. G. Inhibition of the respiratory chain results in a reversible metabolic arrest in *Leishmania* promastigotes. *Mol. Biochem. Parasitol*. **1997**, *85*, 135-138.

44. Wang, C.; Youle, R. J. The role of mitochondria in apoptosis. *Annu. Rev. Genet.* **2009**, *43*, 95-118.

45. Paris, C.; Loiseau, P. M.; Bories, C.; Bréard, J. Miltefosine induces apoptosis-like death in *Leishmania donovani* promastigotes. *Antimicrob. Agents Chemother.* **2004**, 48, 852-859.

46. Lander, N.; Cordeiro, C.; Huang, G.; Docampo, R. Polyphosphate and acidocalcisomes. *Biochem. Soc. Trans*. **2016**, *44*, 1-6.

47. Vercesi, A. E.; Rodrigues, C. O.; Catisti, R.; Docampo, R. Presence of a Na^+/H^+ exchanger in acidocalcisomes of *Leishmania donovani* and their alkalization by anti-leishmanial drugs. *FEBS Lett*. **2000**, *473*, 203-206.

48. López-Martín, C.; Pérez-Victoria, J. M.; Carvalho, L.; Castanys, S.; Gamarro, F. Sitamaquine sensitivity in *Leishmania* species is not mediated by drug accumulation in acidocalcisomes. *Antimicrob. Agents Chemother*. **2008**, *52*, 4030-4036.

49. Luque-Ortega, J. R.; Rivas, L. Miltefosine (hexadecylphosphocholine) inhibits cytochrome C oxidase in *Leishmania donovani* promastigotes. *Antimicrob. Agents Chemother*, **2007**, *51*, 1327-1332.

50. Das, S.; Rani, M.; Rabidas, V.; Pandey, K.; Sahoo, G. C.; Das, P. TLR9 and MyD88 are crucial for the maturation and activation of dendritic cells by paromomycin-miltefosine combination therapy in visceral leishmaniasis. *Br. J. Pharmacol*. **2014**, *171*, 1260-1274.

51. Fernández, M. M.; Malchiodi, E. L.; Algranati, I. D. Differential effects of paromomycin on ribosomes of *Leishmania mexicana* and mammalian cells *Antimicrob Agents Chemother*, **2011**, *55*, 86-93.

52. Maarouf, M.; De Kouchkovsky, Y.; Brown, S.; Petit, P.X.; Robert-Gero, M. *In vivo* interference of paromomycin with mitochondrial activity of *Leishmania*. *Exp. Cell. Res.* **1997**, *232*, 339-348.

53. Cohen, B. E. The role of signaling via aqueous pore formation in resistance responses to amphotericin B. *Antimicrob. Agents Chemother*. **2016**, *60*, 5122-5129.

54. Zhikuan, L.; Twieg, R. J. Copper-catalyzed aryl amination in aqueous media with 2-dimethylaminoethanol ligand. *Tetrahedron Lett*. **2005**, *46*, 2997-3001.

55. Arct, J.; *Przemysl Chemiczny* **1964**, *43*, 332-335.

56. Colmenares, M.; Puig-Kröger, A.; Pello, O. M.; Corb A. L.; Rivas, L. Dendritic cell (DC)-specific intercellular adhesion molecule 3 (ICAM-3)-grabbing nonintegrin (DC-SIGN, CD209), a C-type surface lectin in human DCs, is a receptor for *Leishmania* amastigotes. *J. Biol. Chem.* **2002**, *277*, 36766-36769.

57. Guerrero, E.; Saugar, J. M.; Matsuzaki, K.; Rivas, L. Role of positional hydrophobicity in the leishmanicidal activity of magainin 2. *Antimicrob. Agents Chemother.* **2004**, *48*, 2980-2986.

58. Staderini, M.; Aulić, S.; Bartolini, M.; Ai Tran, H. N.; González-Ruiz, V.; Pérez, D. I.; Cabezas, N.; Martínez, A.; Martín, M. A.; Andrisano, V.; Legname, G.; Menéndez, J. C.; Bolognesi, M. L. A fluorescent styrylquinoline with combined therapeutic and diagnostic activities against Alzheimer's and prion diseases. *ACS Med. Chem. Lett.* **2013**, *4*, 225–229.

59. Schneider, C. A.; Rasband, W. S.; Eliceiri, K.W. NIH Image to ImageJ: 25 years of image analysis. *Nature Methods* **2012**, *9*, 671-675.

Highlights

- A new class of leishmanicidal quinoline derivatives, combining bearing amino chains at C-4 and a styryl group at C-2.
- Some compounds showed low micromolar or submicromolar activity on promastigote and amastigote forms and a good selectivity index.
- Activity due to interference with the mitochondrial activity of the parasite and its bioenergetic collapse by ATP exhaustion.